PHYSICAL REVIEW B VOLUME 26, NUMBER 8 15 OCTOBER 1982

Photoluminescence in a disordered insulator: The trapped-exciton model

S. Kivelson* and C. D. Gelatt, Jr.†
Physics Department, Harvard University, Cambridge, Massachusetts 02138
(Received 2 November 1981; revised manuscript received 3 May 1982)

A simple phenomenological model of the electronic structure of the pseudogap of an amorphous semiconductor is considered, and used as the starting point for a systematic investigation of the processes that determine the nature of the photoluminescence. Many of the most striking features of these materials are shown to derive in a straightforward manner from the nature of the primary luminescing entity, a "trapped exciton" in which the hole is trapped in a localized gap state and the electron is bound to the hole by their mutual Coulomb attraction. Other important properties of the photoluminescence reflect the dynamics of the hopping motion of a charged carrier through a band of localized states.

I. INTRODUCTION

Photoluminescence experiments, which have already proved their power as probes of the electronic structure of crystalline semiconductors,[1–3] have been used extensively in recent years to study the nature of the electronic states in the pseudogap of amorphous semiconductors.[4–13] Often, however, these experiments have been interpreted in an *ad hoc* manner using models that were developed to understand photoluminescence in crystals, with the effects of the noncrystalline nature of the system invoked as needed to obtain agreement between theory and experiment. While many of the concepts introduced in these models are applicable to amorphous systems, there are many important differences between the gap-state structure of amorphous and crystalline semiconductors. Thus, it is useful to study a model that incorporates the disordered character of the amorphous semiconductor from the start, and to consider a broad spectrum of experimental results from the unified perspective of this model. In this paper we derive expressions for the results of various photoluminescence experiments in terms of such a model of a disordered semiconductor.

The conceptual core of a theory of photoluminescence consists of a picture of the process in which the photoexcited electron-hole pair recombines via the emission of light, and a description of the most important nonradiative processes that compete with or quench this luminescence. In the class of models studied here, the luminescing entity is a trapped "exciton" in which one of the charge carriers is trapped in a highly localized state in the pseudogap, and the other carrier is bound to the first by their mutual Coulomb attraction in a large "hydrogenic" state. This hydrogenic state is a photoinduced state in the sense that it owes its existence to the presence of the trapped charge carrier. The radiative recombination rate of the exciton can be quite small because of the large discrepancy in the sizes of the two states produces a small overlap factor.[14] The most important nonradiative process at low temperatures in this class of models is phonon-assisted hopping. Here, the carrier in the large photoinduced state escapes from the vicinity of the trapped carrier by hopping to other localized states elsewhere in the solid. At high temperatures, an additional nonradiative process becomes important in which the carrier in the induced state is thermally activated to the mobility edge and then escapes from the vicinity of the trapped carrier.

The model presupposes a simple picture of the density of one-electron states in the pseudogap, such as the one shown schematically in Fig. 1. The intrinsic density of tailing states (that is, disorder-induced localized states that "tail" into the pseudogap) is taken to be asymmetric, with one band, which we have chosen arbitrarily to be the conduction band, characterized by a relatively sharp band edge and a low density of tailing states while the other (valence) band has a markedly higher density of tailing states. We will consider only the case in which the intensity of the light used to excite the luminescence is sufficiently low that each geminant electron-hole pair (that is, a pair created by the absorption of a single photon) is sufficiently isolated from all others that the effects of other photoexcited electrons and holes can be ignored. Under these conditions, if the gem-

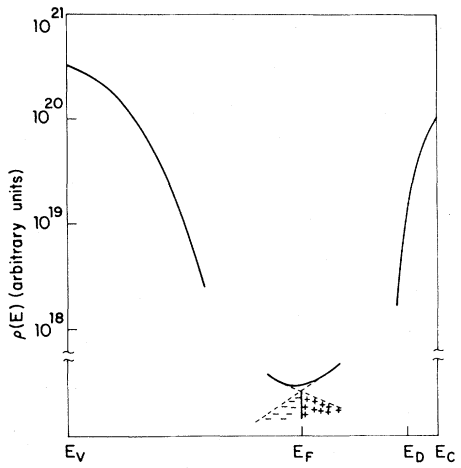

FIG. 1. Schematic density of states of an amorphous semiconductor. Shown here are Gaussian band tails, with a higher density of valence-band than of conduction-band tail states. Also shown, near the center of the pseudogap, are positively charged valence-band-related states above the Fermi level E_F, and negatively charged conduction-band-related states below E_F.

inant electron and hole separate, the luminescence is quenched. The salient features of the model follow directly. The high density of valence-band-related tailing states implies that a hole will become trapped in a localized state almost immediately after excitation. As these states tend to be deep in the pseudogap, the radius of the hole orbital will be rather small. In contrast, the density of conduction-band-related tailing states is low, so the electron remains free much longer and would probably escape from the vicinity of the hole were it not bound to the hole by their mutual Coulomb attraction. Kivelson and Gelatt[15,16] have shown previously that the notion of effective mass can be extended to disordered systems. Thus, if the density of tailing states is not too large, the bound states associated with a charged impurity in a disordered semiconductor are large hydrogenic states with a radius

$$a_B^* \approx \hbar^2 \kappa / m^* e^2 , \tag{1}$$

where, as in the crystal, κ is the static dielectric constant, and m^* is an appropriate average effective mass. For instance, a_B^* is estimated to be approximately 24 Å in a-Si. As the radius of the hole state, in general, is small compared to a_B^*, the bound state of the electron in the field of the hole is similar to that of an electron bound to a charged impurity or defect. Moreover, if the electron orbital is large compared to the correlation length of the disorder, its nature is rather insensitive to the local variations of environment characteristic of disordered systems. Thus, the electron-hole pair forms a trapped "exciton" consisting of a tightly bound hole surrounded by a large hydrogenic electron orbital, and the luminescence results from the radiative recombination of the electron with the hole to which it is bound. This picture of the luminescing entity is the central new concept of this paper and is responsible for many of the most striking predictions of the model. Since there is a wide spread in the properties of the hole states, there will be a wide spread in those properties of the luminescing pairs that depend jointly on the characteristics of the electron and hole orbitals, such as the luminescence energy. Other properties, such as the high-temperature activation energy for ionizing the exciton, which, as we will demonstrate, depend only on the nature of the electron state, will have well-defined values.

In Sec. II the model is described in detail, and the consequences of its structure are explored. It is our purpose in this section to present all the major results of our analysis in general physical terms without recourse to detailed calculations. The dependence of the quantum efficiency on temperature, the strength of an applied external electric field, the intrinsic density of tailing states, and the concentration of charged and neutral impurities is discussed. The time and spectral dependence of the photoluminescence signal is also explained. In particular, the implications of our identification of a trapped exciton as the primary luminescing entity are highlighted.

Many of the quantities invoked in the discussion in Sec. II depend on the statistics of electron or hole hopping motion through a random distribution of localized states. In Sec. III, the results of detailed calculations of these quantities are described. At nonzero temperature, the statistics of the hopping motion of the electrons (or holes) becomes quite complicated. Reliable approximate analytic solutions have been obtained in the low- and high-temperature limits. Many of the results obtained from this analysis are new and should be widely applicable to hopping processes in disordered systems. A particularly interesting new effect predicted by these calculations is that, for certain physically plausible densities of localized states, the low-temperature quantum efficiency is an increasing function of temperature. In other words, we find that under appropriate conditions, the nonradiative process becomes less effective with increasing temperature. In order to obtain re-

liable results at intermediate temperatures and to verify the accuracy of our approximate solutions at low temperatures, a series of computer simulation experiments have been carried out for various choices of the parameters that define the model. The results of these experiments are also discussed.

Finally, in Sec. IV we briefly discuss the implications of the model for interpreting experiment in real amorphous semiconductors. We have previously used the model to make a detailed comparison between theory and experiment in hydrogenated a-Si.[16] However, since there is considerable experimental uncertainty in determining the microscopic parameters which govern the photoluminescence in a-Si, the model must be embellished with a large number of free parameters. Thus, since there is no qualitative result which unambiguously implicates the present excitonic mechanism in the photoluminescence, such a detailed fit to experiment is not useful at this time.

II. THE MODEL

In our model, the nature of the photoluminescence signal derives directly from a simple picture of the intrinsic electronic structure of the pseudogap of the amorphous semiconductor. The density of states is assumed to be of the general form shown schematically in Fig. 1. It is characterized by a valence band and its associated valence-band tail separated from a conduction band and its associated conduction-band tail by a region with a very low density of states. As the Fermi level lies somewhere in midgap, the valence-band-related states are normally full and are charged when empty (when occupied by a hole) while the conduction-band states are normally empty and are charged when occupied. For energies below E_v or above E_c the density of states and carrier mobilities are high (E_v and E_c are often associated with a "mobility edge"). The states between E_v and E_c are said to lie in the pseudogap. In this regime the density of states is small and the carrier mobilities are low since the electronic states are localized and the carriers move via phonon-assisted hopping. On the whole, the further into the pseudogap a state lies, the more localized it becomes. The distribution of tail states is highly asymmetric with a higher density of valence-band tailing states than of conduction-band tailing states. By virtue of their large size, states near the band edges, which includes the greater part of the conduction-band-related states, will tend to be coupled only weakly to the phonon field while the deeper, hence more localized valence-band-related states, may be quite strongly coupled. (Note: The choice of the conduction band as the band with the small density of tailing states is arbitrary. If a system had a density of states with the asymmetric reversed, the physics of the model would remain unchanged with the roles of holes and electrons reversed. However, there is evidence that the density of states pictured in Fig. 1 is qualitatively correct for hydrogenated a-Si.[17])

The presence of a localized positive charge in the solid introduces an associated electron bound state into the system. If the radius of the positive charge density a_+ is small compared to the effective electron Bohr radius [see Eq. (1)], then, regardless of the origin of the charge, the electron bound state will resemble the state of an electron bound to a point charge. In particular if E_D denotes the mean energy of an electron bound to a charged impurity, then the energy of the bound state associated with any other charge will be equal to E_D within core-correction terms of order,

$$\Delta E_{\text{core}} \sim E_{\text{core}}(a_+/a_B^*)^3 , \tag{2}$$

where E_{core} is an energy characteristic of the core potential and is typically of the order of a rydberg. Note that the actual value of E_D relative to the mobility edge E_c, is difficult to estimate theoretically. An effective Rydberg for the hydrogenic state, $\mathscr{R}^* = \hbar^2/2m^*(a_B^*)^{-2}$, can be defined which measures the binding energy of the hydrogenic ground state relative to an effective band edge.[15,16] This energy should not be confused with E_c-E_D, the ionization activation energy, which depends on the location of the mobility edge and is generally expected to be larger than $\mathscr{R}^*$.

In addition to photoexcited holes in traps, localized charges may occur in several ways. There is evidence that a fraction of impurities with valence charge one greater than that of the host element (such as P in a-Si) are incorporated into the amorphous matrix in a singly charged configuration.[17,18] Alternatively, if the valence-band tail overlaps the Fermi level, or if a defect produces a valence-band-derived state above the Fermi level, there will be an intrinsic density of positive charges associated with these empty, highly localized midgap states. A similar hydrogenic bound-hole state is associated with each negative charge in the system, but due to the high density of valence-band tail states, this state is too short lived to be important.

Finally, we need to know enough about the phonon spectrum and the electron-phonon interaction

to permit us to calculate phonon-assisted transition rates between electronic states. The problem is addressed more fully in Appendix A. For now, we will only summarize the most important results of that analysis. Consider two localized states with radius ξ and energies E_1 and E_2, respectively, separated by a distance R. The transition rate γ_{21} is the probability per unit time that an electron (or hole, depending on the nature of the states involved) in state 1 will "hop" to state 2, assuming state 2 is unoccupied. It is convenient to express γ_{21} in the form

$$\gamma_{21}=\gamma(E_1,E_2,R)S(R)\times\begin{cases} e^{-(E_2-E_1)/k_BT} & \text{for } E_2>E_1 \\ 1 & \text{for } E_2<E_1 \end{cases}, \tag{3}$$

where the first term is a frequency that depends on the nature of the phonon field, $S(R)$ is an overlap factor that falls off exponentially at large distances,

$$S(R)\sim e^{-2R/\xi},$$

and the final factor, required by detailed balance, expresses the fact that processes that involve the absorption of phonons (hops up in energy) are less probable than processes involving the emission of phonons. At low temperatures and for small energy differences, $|E_1-E_2|$, γ is well approximated by a constant, γ_0. If we are to treat sites with large energy differences, it is important to include a term that reflects the fact that processes which involve the absorption or emission of many phonons are less probable than processes which involve few phonons. Although γ is in general a rather complicated function, in the case of weak electron-phonon coupling the leading term is of the form

$$\gamma(E_1,E_2,R)\sim\gamma_0 e^{-n}, \tag{4a}$$

where n is the appropriate average of the number of phonons involved in the transition. As large states are coupled most strongly to long-wavelength phonons, the average energy of the relevant phonons is reduced from the Debye energy $\hbar\omega_D$, by a factor of a/ξ, where a is the interatomic spacing, so

$$n\sim|E_1-E_2|/(\hbar\omega_D a/\xi). \tag{4b}$$

Although formally γ_0 is expressed as a product of a number of unknown factors, since it is an attempt frequency it will often be of order ω_D,

$$\gamma_0\sim\omega_D. \tag{4c}$$

In solids with strong electron-phonon coupling, or at high temperature, the detailed functional form of the hopping rate will be more complicated than that contained in Eqs. (3) and (4), making quantitative comparisons with theory difficult. Nonetheless, even in these cases, the simple form in Eqs. (3) and (4) contains the essential physics necessary for a qualitatively correct picture. In particular, it will always be true that small differences in site energies and intersite distances cause enormous changes in the hopping rates. Thus, in a disordered system with a low concentration of localized states (in units of ξ^{-3}), the distribution of hopping rates will be extremely broad and it will be characteristic of the system's statistics that any rate that is larger than some value will tend to be much larger and vice versa. (The distribution of hopping rates at zero temperature for several representative densities of states is illustrated in Fig. 2.)

In terms of the class of models we have just described, we will now discuss the various processes that contribute to the observed luminescence in amorphous semiconductors. We will consider both

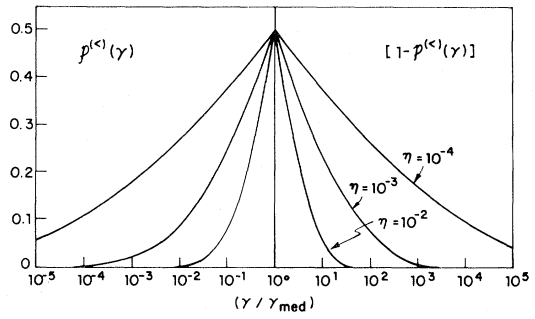

FIG. 2. Distribution of hopping rates about the median rate. γ_{med}, the median hopping rate, is defined in Eq. (19). $\mathcal{P}^{(<)}(\gamma)$, the fraction of sites from which the leaving rate is less than γ, is discussed in Eq. (36). It depends parameterically on the density of available states η, defined in Eq. (37). Notice that even for $\eta=10^{-2}$ the distribution spans over two decades of rates.

steady-state experiments, in which the luminescence is excited by continuous illumination, and transient experiments, in which the luminescence is excited by a brief pulse of light. The fundamental quantity that is measured experimentally is $dI(\hbar\omega,t)$, the intensity of the luminescence radiation with energy $\hbar\omega$ at time t per unit energy, per unit time. In steady-state experiments dI is independent of time,

$$dI(\hbar\omega,t)=dI_{ss}(\hbar\omega) ,$$

while in transient experiments it decays monotonically from the time of the pulse (defined as $t=0$). As a number of distinct processes contribute to the observed luminescence signal, we have broken our discussion into several parts, each dealing with one class of processes. The different classes of processes are illustrated schematically in Fig. 3.

Consider the total steady-state quantum efficiency Y_{tot} (the number of photons emitted per photon absorbed). It can be expressed as a product of two factors,

$$Y_{\text{tot}}=Y_{\text{in}}\bar{Y}_{\text{ex}} , \tag{5}$$

where Y_{in} is the initial probability that an exciton will form following the absorption of a photon, and $\bar{Y}_{\text{ex}}$ is the average probability that the exciton will recombine radiatively once it has formed. Y_{in} is determined by the relaxation processes, discussed in Sec. II A of this section, which take place much faster than any of the other processes discussed here. $\bar{Y}_{\text{ex}}$ is an average over the luminescence spectrum of $Y_{\text{ex}}(\hbar\omega)$, the probability that an exciton with total energy $\hbar\omega$ will recombine radiatively. The luminescence spectrum is determined by the distribution of hole energies. As described in Sec. II B, this distribution depends upon the dynamics of the hole thermalization process in which a trapped hole loses excess energy via phonon-assisted hopping between valence-band-tail states. The competition between the radiative and nonradiative processes which can destroy an exciton determines $Y_{\text{ex}}(\hbar\omega)$. In Sec. II C, the rate of radiative decay of an exciton is calculated as a function of the radius of the hole wave function. As several workers in the field have analyzed their data in terms of donor-acceptor-type recombination, we also calculate the rate at which this process occurs, and conclude that exciton recombination is the more important radiative mechanism for the class of models considered here. Since, by assumption, all radiative recombination is geminant, the most important nonradiative processes are those that allow the electron to escape from the vicinity of the hole. Section II D is devoted to these processes. At low temperatures phonon-assisted hopping through conduction-band-tail states is the most important of these, while at higher temperatures it becomes possible for the electron to escape via activation to the "mobility edge" E_c. The overall behavior of the luminescence signal $dI(h\omega,t)$, encompassing the combined effects of all the individual processes explored in Secs. II A–II D, is also discussed at this point. Section II D concludes with a brief study of the limits the condition that all radiative recombination be geminant places on the intensity of the radiation used to excite the luminescence. Finally, in Sec. II E the consequences of additional perturbations of the system are considered. Some of the effect on the luminescence signal of an applied electric field is discussed, as well as the effect of a given concentration of charged or neutral impurities.

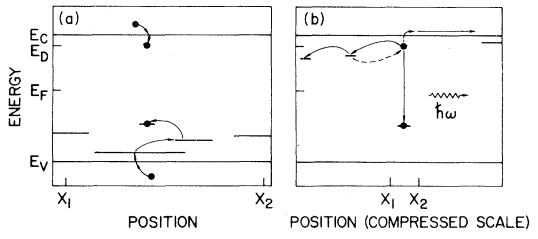

FIG. 3. Schematic representation of the processes that contribute to the luminescence. (a) Initial relaxation: The photogenerated electron and hole relax to the band edge by emitting phonons. The hole is then trapped in a localized valence-band tail state and the electron is bound to it in an induced excitonic state. The dynamics of these initial relaxation processes determines the initial exciton-formation probability Y_{in}. Hole thermalization: The hole hops through the valence-band tail toward the Fermi level until it becomes trapped in a state sufficiently isolated that no more hopping occurs on the time scale of the problem. The dynamics of the hole thermalization determines the luminescence spectrum. (b) Radiative recombination: The electron and hole which form the exciton can recombine accompanied by the emission of a photon with energy $\hbar\omega$. Nonradiative exciton ionization: The luminescence is quenched when the electron escapes from the bound state induced by the hole. At zero temperature the electron can escape by hopping to a neighboring conduction-band tail state with energy less than E_D. At low temperatures it becomes possible for the electron to hop away and then back. At still higher temperatures the electron can escape via direct thermal activation to the mobility edge E_c.

A. Relaxation to the band edges

The total quantum efficiency is proportional to an initial exciton formation probability Y_{in}, which is determined by the dynamics of the initial relaxation processes. Y_{in} is the product of two factors: (i) the probability that, while relaxing to the mobility edges, the electron and hole will not become too widely separated to permit exciton formation, and (ii) the probability that an exciton will form once the electron and hole have relaxed to the mobility edges. The photoluminescence is usually excited by the absorption of a photon with energy E, well in excess of $E_{\text{gap}} \equiv E_c - E_v$, so the electron and hole initially have considerable kinetic energy. As they relax to the mobility edges by emitting phonons, they diffuse apart a characteristic distance $l_{\text{relax}}(E - E_{\text{gap}})$ which depends on the excess kinetic energy [shown schematically in Fig. 3(a)]. If the electron-hole pair separate by a distance greater than about a_B^*, then the exciton will not form and there will be no luminescence. If we assume that the electron travels an average distance $\bar{l}$ with each phonon emission event, then a crude estimate of l_{relax} can be obtained[19]:

$$l_{\text{relax}} \sim \left[\frac{\bar{l}^2 n(E)}{2} \right]^{1/2} ,$$

where $n(E) \sim (E - E_c)/\hbar\omega_D$ is the mean number of phonons emitted, and $\bar{l}$ is expected to be of order an interatomic spacing.

An electron and hole that have relaxed to the mobility edge within about a_B^* of one another can form an exciton. In order to conserve energy, exciton formation must be accompanied by the emission of phonons. The rate ν_{ex} at which this process occurs may depend, to some extent, on the nature of the states at the mobility edge but a fairly reliable estimate of ν_{exc} can be obtained on the basis of Eq. (4),

$$\nu_{\text{exc}} \sim \omega_D e^{-n} , \tag{6a}$$

where $n \sim (E_c - E_D)/(\hbar\omega_D a/a_B^*)$ is the average number of phonons involved in the transition. Note that ν_{exc} is related to the rate of exciton ionization ν_{ac} [see Eq. (21)] by the condition of detailed balance. It is also possible for the electron and hole to escape from each other via the absorption of a phonon. If, as before, l_{relax} is the typical separation between the electron and hole, then their binding energy is determined by their mutual Coulomb attraction, so according to Eqs. (3) and (4) the escape process is characterized by a rate[20]

$$\gamma_{\text{escape}} \sim \omega_D e^{-\epsilon_{\text{in}}/k_B T} , \tag{6b}$$

where

$$\epsilon_{\text{in}} \sim e^2/\kappa l_{\text{relax}} . \tag{6c}$$

In most cases of interest, the excitation energy will be chosen sufficiently low such that $l_{\text{relax}} < a_B^*$, so ϵ_{in} will be somewhat greater than the effective Rydberg $\mathscr{R}^*$.

Combining these results, an approximate expression for Y_{in} as a function of excitation energy[20] is obtained:

$$Y_{\text{in}}(E) \sim \left[\frac{1}{1 + (l_{\text{relax}}/a_B^*)^3} \right] \left[\frac{\nu_{\text{ex}}}{\nu_{\text{exc}} + \gamma_{\text{escape}}} \right] . \tag{7}$$

Once the exciton has formed, all memory of the excitation process is lost. Y_{in} is the only quantity that depends on excitation energy. Furthermore, the initial relaxation processes are all much faster than the processes discussed subsequently. (The slowest rate discussed above is ν_{exc}, which typically is 2 or 3 orders of magnitude less than ω_D, hence $\nu_{\text{ex}} \sim 10^{10} - 10^{11}$ sec^{-1}.) Thus, for the purposes of the following discussions, the initial relaxation processes are viewed as instantaneous, and the origin of time is taken to be the moment of exciton formation.

B. Hole thermalization

After the initial relaxation is completed, the electron and hole have energies approximately equal to E_c' and E_v, respectively, and are bound to each other by their mutual Coulomb attraction in a state of radius a_B^*. Owing to the presence of tailing states, they are each subject to trapping in intrinsic localized states. This occurs much more rapidly for the hole due to the asymmetry of the density of localized states. Since the density of localized states decreases rapidly as a function of energy above the band edge, most of the holes initially fall into localized states with energy near E_v. The holes then gradually thermalize toward midgap via phonon-assisted hops between tail states as shown schematically in Fig. 3(a), so the time-dependent spectral distribution of the holes, $p_v(E,t)$, gradually broadens and shifts toward midgap. As this process proceeds, the holes find their way to more and more isolated sites, and the hopping rates become progressively slower until no more motion occurs on the time scale of interest.

On the whole, the deeper lying the localized state, the longer a hole remains trapped in it, both because deeper lying states are more strongly localized than band-edge states, and because there is a smaller density of tail states with comparable or lower energy to which the hole can hop readily. Thus, the spectral distribution of holes is determined by a competition between the falling density of tail states and the increasing median lifetime of those states as a function of energy above E_v.

Consider the fate of the holes that are excited by a burst of light at time zero (transient photoluminescence). Since there is such a broad distribution of hopping rates, at any time $t \gg \gamma_0^{-1}$ essentially all the holes will be trapped in states from which the leaving rate is less than t^{-1}. Thus, at times short compared to the radiative lifetime, the spectral distribution of holes will be approximately equal to the distribution of such "slow" states,

$$P_v(E,t)=\frac{\rho_v(E)\mathscr{P}_v^{(<)}(E,t^{-1})}{\int d\epsilon\,\rho_v(\epsilon)\mathscr{P}_v^{(<)}(\epsilon,t^{-1})} , \tag{8}$$

where $\rho_v(E)$ is the density of valence-band tailing states and $\mathscr{P}_v^{(<)}(E,t^{-1})$ is the probability that the leaving rate from a hole state with energy E is less than t^{-1}. [$\mathscr{P}_v^{(<)}(E,t^{-1})$ is calculated explicitly in Sec. III E.] The broad dispersion in leaving rates also implies that if a hole is in a given localized state at time t, it has probably been there for most of its life. Since the energy of the electron in the exciton is always approximately E_D the energy of the recombination radiation is

$$\hbar\omega = E_D - E_{\text{hole}} . \tag{9}$$

Thus, the luminescence spectrum is determined by $P_v(E,t)$,

$$dI(\omega,t) \propto \nu_{\text{rad}}(\omega) P_v(E_D-\hbar\omega,t) , \tag{10a}$$

where $dI(\omega,t)$ is the luminescence intensity per unit frequency range per unit time, and $\nu_{\text{rad}}(\omega)$ is the mean radiative decay rate of an exciton with total energy $\hbar\omega$. Similar considerations lead to an expression for the steady-state luminescence spectrum,

$$dI_{ss}(\omega) \propto \nu_{\text{rad}}(\omega) P_v(E_D-\hbar\omega,\nu_{\text{rad}}^{-1}) . \tag{10b}$$

Since the holes are trapped in such "slow" sites, the hole distribution does not change very much over the entire range of radiative lifetimes ν_{rad}^{-1}, and the frequency dependence of the argument ν_{rad}^{-1}, in Eq. (10b), is relatively unimportant.

The simple argument that led from Eq. (8) to Eqs. (10) may be somewhat complicated by phonon broadening. Equation (9) embodies the assumption that the energy of the emitted photon is always equal to the total excess energy of the exciton. However, as the hole states are small, they tend to be rather strongly coupled to the phonon field, hence processes in which the photon emission is accompanied by the absorption or emission of phonons are possible. This results in a broadening of the spectrum that is proportional to the deformation potential.[10] Nonetheless, because the valence-band tail is often quite broad compared to a typical phonon energy $\hbar\omega_D$, the photoluminescence spectrum can still be derived approximately from Eqs. (10) in some materials. Evidence that this is the case for a-Si will be presented in Sec. IV.

The size of the localized-tail states is generally a decreasing function of their binding energies. It has been shown[21] that for tail states in heavily doped crystalline semiconductors, the energy dependence of the radius of a tail state is similar to that normally expected for shallow states in the band gap of a nearly perfect crystal,

$$a_{\text{hole}} = a_{\text{tail}}(E) \sim (E-E_v)^{-1/2} . \tag{11a}$$

So long as the radius of the tail state is larger than the correlation length of the disorder, this relation should hold for the tail states in an amorphous semiconductor as well.

In the opposite extreme, when the size of the states is comparable to an interatomic spacing a, the state radius is determined by the length scale of the potential fluctuations, and is roughly independent of the binding energy of the state. Such states resemble the deep-impurity or defect-related states found in crystals, in that they tend to be associated with a particular atomic scale "defect":

$$a_{\text{hole}} = a_{\text{def}}(E) \sim a . \tag{11b}$$

The two types of localized states can coexist, since different types of potential fluctuations can lead to bound states with the same binding energy but different radii. Evidence that "true" valence-band tail states and valence-band defect states coexist in a-Si will be presented in Sec. IV.

C. Radiative recombination

The radius of the hole state determines the rate of radiative recombination. Radiative recombination is a generic term for processes in which an electron in an excited state makes a transition to an unoccupied, lower-lying state (annihilates a hole) accompanied by the emission of a photon.

So long as the electron-phonon coupling is not too great, the radiative transition rate is derived simply from Fermi's golden rule,[22]

$$\hbar\nu_{\rm rad}(\omega)=\kappa^{1/2}\frac{(\hbar\omega)^3e^2|\langle i|x|f\rangle|^2}{3\hbar^3c^3} \tag{12}$$

where $\hbar\omega$ [$\hbar\omega=$ (initial energy)$-$(final energy)] is the energy of the photon, κ is the static dielectric constant of the medium, c is the speed of light, and $\langle i|x|f\rangle$ is the dipole-matrix element between the initial state and final states. For the present model of the exciton, the initial state is a large hydrogenic bound state with radius a_B^* and the final state is a trapped-hole state with a much smaller radius $a_{\rm hole}$ [see Fig. 3(b)]. Although the precise value of the dipole-matrix element depends on the details of the disorder potential in the vicinity of the hole, the square of the matrix element will in general consist of an overlap term S, which is approximately proportional to $(2a_{\rm hole}/a_B^*)^3$ times the squared dipole moment of the smaller state,

$$|\langle i|x|f\rangle|^2\sim S_{\rm if}\langle f|x^2|f\rangle\ . \tag{13a}$$

If the hole wave function is roughly the size of an atomic scale defect, then within an order of magnitude uncertainty,

$$|\langle i|x|f\rangle|^2\sim\frac{(2a_{\rm hole})^5}{(a_B^*)^3}\ . \tag{13b}$$

As the expression is proportional to the fifth power of the hole radius, this uncertainty can be regarded as a 50% ambiguity in the proper definition of the appropriate hole radius. It should be noted that the approximations that lead to the expressions in Eqs. (13) are only rigorously justifiable when $a_{\rm hole}$ is not much larger than an interatomic spacing, since if the hole state is large, the effect of the underlying structure of the unperturbed valence- and conduction-band-edge states becomes important. This limit is also considered in Appendix B. Nonetheless, in this paper we will use Eq. (13b) whenever we need to estimate a dipole-matrix element. For large hole states, this may result in a slight overestimate of the associated radiative decay rate, but the results are still expected to be qualitatively correct.

Despite the uncertainty, considerable useful information can be obtained from Eq. (12). First, information about the size of the hole states can be used to make an estimate of the radiative rate and, in particular, to predict the frequency dependence of the radiative rate. This frequency dependence consists of the explicit ω^3 part and an implicit part due to the dependence of $a_{\rm hole}$ on the hole binding energy,

$$\nu_{\rm rad}(\omega)\propto(\hbar\omega)^3a_{\rm hole}^5(E_d-E_v-\hbar\omega)\ , \tag{14}$$

where $E_d-E_v-\hbar\omega$ is the hole binding energy. Conversely, it is often possible to measure the radiative decay rate as a function of energy and, by reasoning backward from Eq. (13), to estimate the size of the relevant hole states.

In doped crystalline semiconductors, the donor-acceptor model of radiative recombination has had notable success in explaining the results of photoluminescence experiments,[1,3] and it has been suggested that a similar mechanism might be responsible for the luminescence in amorphous semiconductors as well. In this model, the electron and hole occupy separate localized states and recombine via radiative tunneling (RT). The rate at which this process occurs can be estimated on the basis of the same considerations that led to Eqs. (12) and (13). In the case of radiative tunneling there is an extra overlap factor which depends exponentially on the separation R between the electron and hole

$$[S_{fi}]_{\rm RT}\sim e^{-2R/a_B^*}[S_{fi}]_{\rm exc}\ .$$

Thus, if R_0 is the median separation between nearest-neighbor electron-tail states, the rate of donor-acceptor recombination will be smaller than the rate for exciton recombination by a factor of order e^{-2R_0/a_B^*},

$$(\nu_{\rm rad})_{\rm RT}\sim e^{-2R_0/a_B^*}[\nu_{\rm rad}]_{\rm exc}\ . \tag{15}$$

Donor-acceptor recombination is observed in doped crystals because the localized donor and acceptor states are neutral when occupied by an electron or hole, respectively, so that trapped excitons of the sort considered here do not form. However, if the localized tail states are charged when occupied, as they generally are believed to be in amorphous semiconductors, excitons can form. Since radiative tunneling is far slower than "exciton" recombination, the latter process dominates.

D. Nonradiative electron processes including phonon-assisted hopping

At any time t the intensity of the luminescence radiation per unit time per unit energy is proportional to the number of excitons with energy $\hbar\omega$,$dN(\omega,t)$:

$$dI(\omega,t)=\hbar\omega\nu_{\rm rad}(\omega)dN(\omega,t)\ . \tag{16}$$

Following the creation of an ensemble of excitons, three processes tend to affect the number of excitons with energy $\hbar\omega$: (i) The hole thermalization processes described in Sec. II B change excitons of energy $\hbar\omega$ into excitons of energy $\hbar\omega'$. (ii) Each radiative transition of the sort described in the last section annihilates an exciton. (iii) The nonradiative processes in which an electron is separated from the hole to which it was bound (exciton ionization) are competitive with the radiative process since, by assumption, all radiative recombination is geminant [see Fig. 3(d)]. The first two processes depend on the nature of the hole state and on the structure of the valence-band tailing states, but are insensitive to the nature of the conduction-band tail states. On the other hand, the nonradiative electron processes are insensitive to the nature of the hole orbital (so long as $a_{\text{hole}} \ll a_B^*$), but often depend critically on the local configuration of the conduction-band tail states. As the hole thermalizes, it diffuses a distance of order a few times the median separation between nearest-neighbor valence-band tail states. This distance is small compared to the typical separation between conduction-band tail states in the case of a "highly asymmetric" density of states. In this case, the electron follows the hole motion adiabatically, and the local configuration of conduction-band tail states accessible to the electron does not change appreciably as the hole hops. The electron- and hole-hopping processes are thus independent of each other.[23] If the asymmetry in the density of states is less pronounced, the local configuration of conduction-band tail states does change; the electron- and hole-hopping processes are coupled and must be treated on an equal footing. For the sake of simplicity of development, in this section we will treat only the first case.

If N_0 photons per unit area with energy E were absorbed at time zero, then

$$dI(\omega,t)/N_0 = Y_{\text{in}}\nu_{\text{rad}}(\omega)\hbar\omega \times P_v(E_D - E_v - \hbar\omega, t)G_c(\hbar\omega,t) , \tag{17}$$

where Y_{in} is the initial probability that an exciton will form, as in Eq. (6), P_v is the hole spectral distribution at time t given by Eq. (8), and $G_c(\hbar\omega,t)$ is the probability that an electron that is bound to a hole at time zero is also there at time t. G_c depends on the total energy of the exciton $\hbar\omega$ only through radiative decay rate $\nu_{\text{rad}}(\omega)$. Similarly, the steady-state quantum efficiency is determined by the average over the steady-state spectrum of the probability $Y_{\text{ex}}(\hbar\omega)$, that an exciton with total energy $\hbar\omega$ will recombine radiatively. This is expressed in Eq. (5) where

$$\bar{Y}_{\text{ex}} = \int d\epsilon\, P_v(E_D - E_v - \epsilon, \nu_{\text{rad}}^{-1}) Y_{\text{ex}}(\epsilon) , \tag{18a}$$

P_v is given by Eq. (10b), and

$$Y_{\text{ex}}(\hbar\omega) = \int_0^\infty dt\, G_c(\hbar\omega,t) . \tag{18b}$$

At low temperatures the dominant ionization mechanism is phonon-assisted hopping of the electron from the hole-induced state to a nearby conduction-band-tail state. The details of this hopping problem are studied in Sec. III and Appendix C. For now, we will just make some general observations. This process is characterized by a broad distribution of rates. Some excitons have near-neighbor conduction-band tail states and are characterized by a fast ionization rate while others have only relatively far neighbors and have a correspondingly slow ionization rate. The ionization rate is very sensitive to the density of electron tailing states. For instance, at zero temperature, the median hopping rate γ_{med} is determined by the mean density η of conduction-band tail states with energy less than E_D,

$$\gamma_{\text{med}} = \gamma_0 e^{-(\ln 2)^{1/3} 2R_0/a_B^*} , \tag{19}$$

where $R_0 = (4\pi\eta/3)^{1/3}$. The quantum efficiency is about $\frac{1}{2}$ when $\gamma_{\text{med}} = \nu_{\text{rad}}$. The temperature dependence of the hopping process is quite complicated and depends sensitively on the density of tailing states. In general, variations will take place over a temperature range T_0, characteristic of variations in the integrated density of conduction-band tail states

$$k_B T_0 = \left| \frac{d}{dE_D} \ln \int^{E_D} dE\, \rho(E) \right|^{-1} . \tag{20}$$

To determine whether the quantum efficiency increases or decreases as the temperature is raised from zero is a subtle problem. As the temperature increases, more localized states become accessible since the electron can hop to states with energy greater than E_D. This tends to increase the typical ionization rate, or decrease the quantum efficiency. At finite temperatures it also becomes possible for an electron that has hopped away from the hole to hop back again. This effect tends to increase the quantum efficiency. The balance between the two

effects depends on the magnitude and shape of the density of states in the vicinity of E_D. Two important cases are explored in detail in Sec. III. If the concentration of charged defects in the material is small, the density of states will be smooth in the neighborhood of E_D as in Fig. 4(a). In this case, the quantum efficiency is an increasing function of temperature for samples with a relatively low density of tail states (zero-temperature quantum efficiency $\gtrsim 0.4$) and a constant or decreasing function of temperature for samples with a higher density of tail states. If the concentration c_+ of charged defects in the material is large, there will be a peak in the density of states centered on E_D as in Fig. 4(b). If we denote the spread in energies of the bound states associated with these defects by ΔE_D, the height of the peak will be approximately $c_+/\Delta E_D$.[24] The narrowness of this peak in the density of states means that the electron never hops to a state with energy much less than E_D, so the effect of hop back is more pronounced in this case. Thus, even in samples in which, due to the presence of charged defects, the zero-temperature quantum efficiency is much less than 0.4, the quantum efficiency will tend to increase as a function of temperature. A detailed discussion of the low-temperature quantum efficiency is contained in Sec. III C.

At higher temperatures it is possible for the electron to be thermally activated to the mobility edge

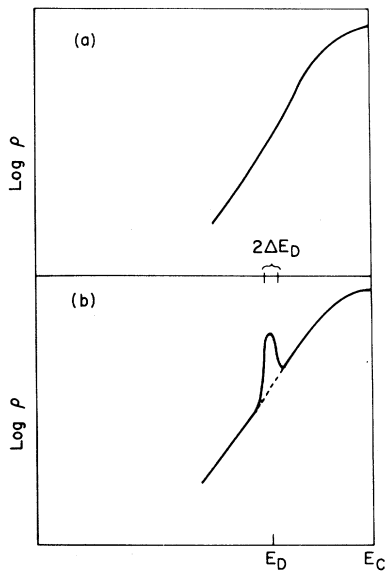

FIG. 4. Schematic representation of the conduction-band tail density of states, (a) when the concentration of charged defects is small, and (b) when it is large.

E_c, where it can escape from the vicinity of the hole. The rate of ionization ν_{ac} is given approximately by the semiclassical expression

$$\nu_{ac} \sim \nu_{\text{exc}} e^{-(E_c - E_D)/k_B T} , \tag{21}$$

where ν_{exc} is a temperature-independent attempt frequency and the temperature-dependent factor reflects the probability of a thermal fluctuation of sufficient magnitude to elevate the electron to E_c. As mentioned previously, ν_{exc} is the rate of exciton formation and is given by the expression in Eq. (6a).

Throughout this discussion, we have tacitly assumed that so long as the electron remains bound to the hole, it can only recombine radiatively. Of course, there always exists the possibility that the electron and hole will recombine nonradiatively even if the exciton is not ionized. Because this process involves the emission of many phonons, it is generally quite slow, due to the exponentially small probability of multiphonon processes. The same analysis that led from Eqs. (3) and (4) to Eqs. (16), yields the nonradiative recombination rate of an exciton with total energy $\hbar\omega$,

$$\nu_{\text{nonrad}}(\hbar\omega) \sim \gamma_0 (2a_{\text{hole}}/a_B^*)^3 e^{-n} , \tag{22a}$$

where n is the number of phonons emitted in the process,

$$n \gtrsim E_{\text{gap}}/\hbar\omega_D , \tag{22b}$$

and the term in parentheses is the same overlap factor that appears in Eqs. (12) and (13) for the radiative recombination rate. Since the pseudo-band-gap is usually much greater than the Debye energy, this rate is generally much smaller than the radiative rate. (The effect of high-energy optical-phonon modes is discussed in Appendix A.)

Finally, to complete our understanding of the nonradiative processes, we must examine the fate of the electron and hole once they have been separated. Nonradiative recombination, even in crystalline semiconductors, is a poorly characterized phenomenon; thus it is not surprising that we can do little more than make some general observations. We must answer one simple question: Given that an electron has escaped from a hole, will it somehow trickle down to the Fermi level via nonradiative processes before it encounters another hole with which it can recombine radiatively? Because of the low probability of transitions involving the emission of many phonons, nonradiative recombination is expected to proceed most efficiently at recombination centers, defect sites with associated midgap states. That this is usually the

case in crystals.[25] even with relatively low defect concentrations, strongly supports this contention. So long as the density of these recombination centers is greater than the density of excitons, an electron will on the average encounter a recombination center before it encounters a nongeminant hole with which it can recombine radiatively. Thus, whenever the intensity of the exciting light is low enough that the density of excitons is less than that of recombination centers, most of the radiative recombination is geminant.[26]

E. Other effects

Additional insight into the photoluminescence mechanisms can be gleaned from experiment by introducing additional perturbations into the system. In particular, the luminescence can be studied as a function of applied-electric-field strength, doping level, and the content of other impurities (such as H in a-Si). All of these can be introduced into the model quite simply.

An electric field can facilitate the exciton ionization process in which the electron escapes via excitation to the "mobility edge." The major effect of an electric field of magnitude F is to alter the activation energy in Eq. (21a), so that

$$\nu_{ac} \sim \nu_{\rm exc} e^{-[E_c - E_D - \delta(F)]/k_B T} , \tag{21a}$$

where $\delta(F)$ is the field-induced change in the activation energy, frequently approximated by the Poole-Frankel expression,[27]

$$\delta(F) = -\beta\sqrt{F} ,$$

with

$$\beta = 2e^{3/2}/\sqrt{\kappa} .$$

The major effect of doping with either donors or acceptors is to raise the density of localized states with energies in the vicinity of E_D, and hence to decrease the quantum efficiency. Whenever a positively charged defect is introduced into the system, a new localized state with energy $\sim E_D$ appears associated with it. A donor directly introduces such a charge into the system but an acceptor does as well since, by the condition of charge neutrality, when a negatively charged impurity is placed in the system, it must be accompanied by a positively charged hole. This hole appears at the Fermi level in a midgap highly localized state, and behaves as a point charge. In other words, whenever a new localized charge of one sign is introduced into the system, a localized charge of the opposite sign is introduced as well. We have, to this point, tacitly ignored the effect of the negatively charged centers in the system. However, because of the asymmetry in the density of intrinsic tail states, the effect of these negative charges will only become important at such high densities that any photoluminescence will already have been quenched by the presence of so many positive charges.[28]

The possible effects of neutral impurities can be manifold, and depend on the nature of the impurity. One possibility is that the presence of impurities can influence the activation energy of the electron to the mobility edge $E_{ac} = E_c - E_D$. Consider the case in which with each impurity atom introduced into the solid, there is an associated state near the conduction-band edge. An example of such an impurity might be hydrogen in a-Si, since there is evidence[29] that the Si-H antibonding states normally lie just above the conduction-band edge. To be concrete, suppose that the impurity potential H' can be written approximately in tight-binding notation,

$$H' = |A_{\rm im}\rangle V \langle A_{\rm im}| ,$$

where $|A_{\rm im}\rangle$ is the impurity-related state with energy $E_{\rm im}$. If there are, on the average, many such impurities within a volume $(a_B^*)^3$, there will be no change in the activation energy E_{ac}, to first order in V, since the first-order shifts of E_c and E_D are equal. Thus if $E_{ac}^{(0)}$ equals the value of $E_c - E_D$ in the absence of impurities, then in the presence of impurities

$$E_{ac} = \tfrac{1}{2}\{E_{ac}^{(0)} - (E_{\rm im} - E_c) + [(E_{ac}^{(0)} + E_{\rm im} - E_c)^2 + 4n_{\rm im}V^2]^{1/2}\} ,$$

where $n_{\rm im}$ is the number of impurities that interact with the hydrogenic electron state,

$$n_{\rm im} \approx \frac{4\pi(a_B^*)^3}{3} c_{\rm im} ,$$

and $c_{\rm im}$ is the mean concentration of impurities. Therefore, at low concentrations, the shift in the activation energy is proportional to the concentration of impurities, while at higher concentrations it is proportional to the square root of the concentration.

III. HOPPING IN A DISORDERED SYSTEM

In this section we calculate explicitly the various quantities discussed in Sec. II that depend on the statistics of hopping motion in a disordered sys-

tem. We focus primarily on the motion of the electron subsequent to its being trapped in the state induced by a hole. At temperatures sufficiently low that direct thermal ionization to the mobility edge is unlikely, the dominant mechanism by which the electron can escape from the hole is phonon-assisted hopping. Thus, many characteristics of the photoluminescence, notably the temperature dependence of the quantum efficiency and the time dependence of the luminescence signal, are determined largely by the statistics of the electron's hopping motion. Hole thermalization also proceeds via phonon-assisted hopping, so the spectral dependence of the luminescence is determined in large measure by the hopping statistics of the holes.

The plan of this section is as follows. In Sec. III A we develop a general formalism for treating hopping problems and derive various exact results. Although certain characteristics of the zero-temperature hopping problem can be calculated exactly by these techniques, at finite temperature the problem becomes far more complicated and approximations must be introduced in order to make further progress. In Sec. III B we introduce the greatest rate approximation (GRA) which is useful at low temperatures. In particular, we use the GRA to compute the quantum efficiency as a function of temperature at low temperatures. Then, in Sec. III C, we introduce the typical rate approximation (TRA) to estimate the quantum efficiency at higher temperatures. In order to test the validity of these approximations we have performed a series of numerical simulation experiments on model hopping systems. In Sec. III D, these experiments are described and their results are used to verify the accuracy of results obtained for the same model using the aforementioned approximations. Many of the concepts developed in Secs. III A–III D are common to a broad class of phenomena in disordered insulators, so we have adopted a formalism that is applicable to the class in general. However, it is conceptually simpler to discuss the underlying physics with a specific example in mind. Thus, in Secs. III A–III D we have considered those aspects of the theory necessary to understand the electron hopping processes.

Finally, in Sec. III E we consider the problem of hole thermalization. The same basic considerations that were developed in the context of the electron hopping problem are applicable to holes as well. However, the problem of hole thermalization is somewhat more complicated because we must keep track of the distribution of hole energies, not just the site occupation statistics. We are thus forced to use a somewhat less systematic approach.

Since the actual calculations of the quantities discussed here are rather lengthy, they have been relegated to Appendix C. In the present section we discuss the results of those calculations and the important physical concepts they illustrate.

A. Formal considerations and exact results

In order to facilitate the discussion, we label each localized state by its location $\vec{R}$, so that we can think of the hopping entity as executing a complicated time-dependent random walk by hopping from site to site. This motion is described quite generally by the set of time-dependent site occupation probabilities $\mathcal{P}_{\vec{R}}(t)$, which obey the equation of motion

$$\frac{d\mathcal{P}_{\vec{R}}}{dt} = -(\nu_{\vec{R}} + \Gamma_{\vec{R}})\mathcal{P}_{\vec{R}} + \sum_{\vec{R}'} \gamma_{\vec{R}\,\vec{R}'}\mathcal{P}_{\vec{R}'} , \tag{23a}$$

where $\gamma_{\vec{R}\,\vec{R}'}$ is the hopping rate from site $\vec{R}'$ to site $\vec{R}$, $\Gamma_{\vec{R}}$ is the total hopping-away rate from site $\vec{R}$ to any other site,

$$\Gamma_{\vec{R}} = \sum_{\vec{R}'} \gamma_{\vec{R}'\,\vec{R}} , \tag{24}$$

and $\nu_{\vec{R}}$ is the rate at which electrons are lost from site $\vec{R}$ by processes other than hopping. Thus $\nu_{\vec{R}} + \Gamma_{\vec{R}}$ is the total loss rate from site $\vec{R}$. In a pure hopping problem, $\nu_{\vec{R}} = 0$ for all sites, which ensures conservation of probability. However, we want to include processes such as radiative recombination, that do not conserve the number of electrons.

To be concrete, we will consider a system in which the hopping entity is an electron that initially is bound to a hole at the origin (site $\vec{0}$) and has the possibility of hopping away through a random distribution of localized states. Thus, the site occupation probabilities are subject to the initial condition

$$\mathcal{P}_{\vec{R}}(0) = \delta_{\vec{R}\,\vec{0}} , \tag{23b}$$

and the rates at which electrons are lost by other than hopping processes are

$$\nu_{\vec{0}} = \nu_{ac} + \nu_{\rm rad} \tag{25}$$

and

$$\nu_{\vec{R}} = \nu_{ac} \quad \text{for } \vec{R} \neq \vec{0} ,$$

where ν_{rad} is the radiative decay rate of the exciton, ν_{ac} is the rate at which electrons are thermally activiated to E_c [see Eq. (21)]. and we have assumed that once this occurs, the electron inevitably escapes from the vicinity of $\vec{0}$ and is out of the problem.

Since luminescence is only possible when the electron is bound to the hole (is on site $\vec{0}$), an important quantity is $\mathcal{G}_{\vec{0}}(t)$, the probability that an electron that was initially on site $\vec{0}$ is also there a time t later. $\mathcal{G}_{\vec{0}}(t)$ depends sensitively on the configuration of neighboring sites. If there is a site $\vec{R}$ close to site $\vec{0}$, the electron can hop to site $\vec{R}$ rather easily, so $\mathcal{G}_{\vec{0}}(t)$ will decay rapidly from its initial value of one. If the site $\vec{0}$ is relatively isolated, then $\mathcal{G}_{\vec{0}}(t)$ will decay much more slowly. The quantities of experimental interest can all be calculated in terms of the configuration average of $\mathcal{G}_{\vec{0}}$, denoted by $\langle \mathcal{G}_{\vec{0}}(t) \rangle$. For instance, the average probability $G_c(\hbar\omega,t)$, that an electron which was initially bound to a hole with energy $E_D - \hbar\omega$ is there a time t later [invoked in Eqs. (17) and (18)], is given by the expression

$$G_c(\hbar\omega,t) = \langle \mathcal{G}_{\vec{0}}(t) \rangle_{\nu_{\vec{0}} = \nu_{\text{rad}}(\omega) + \nu_{ac}} , \tag{26}$$

where the entire dependence on $\hbar\omega$ is contained in the radiative recombination rate. The average probability that the same electron will recombine radiatively at some time $Y_{\text{ex}}(\hbar\omega)$ is expressed in terms of G_c in Eq. (18b).

Unlike the more usual random-walk problems, where interest focuses on transport phenomena that depend on the long-range behavior of the hopping motion, the problems considered here depend on the random walk over short distances, since once the electron has escaped from the immediate vicinity of the hole, it has little chance of ever returning to it.

To complete the formal definition of the hopping problem, we must prescribe the ensemble of hopping rates $\gamma_{\vec{R}\,\vec{R}'}$. In other words, we must make some assumptions about the density of localized states and the hopping rates between them. We focus our attention on two classes of systems. Naively, one would expect the density of conduction-band tail states $\rho_c(E)$, to be a smooth function of energy and featureless in the vicinity of E_D as pictured in Fig. 4(a). In this case, we will see that the small differences in the Coulombic binding energies of the electrons bound to holes in different local environments, ΔE_D in the figure, are unimportant and can be ignored without significant error. Thus, the energy of the state at site $\vec{0}$ can be treated as a configuration-independent quantity, E_D. More generally, the variations in the electron energies can be important and all quantities must be averaged over the distribution $D_{\text{Coul}}(E)$ of electron Coulombic binding energies. Note that this distribution of electron binding energies is not to be confused with the distribution of *total* exciton energies which is largely determined by the spread in *hole* energies. Averaging over D_{Coul} is especially important if the density of states is also peaked in the vicinity of E_D as shown in Fig. 4(b). A peaked density of this form will, in fact, be found in any amorphous semiconductor with a high density of charged defects since each positive charge induces an electron bound state with energy within about ΔE_D of E_D. Thus, the density of states is the sum of a featureless density of "intrinsic" tail states $\rho_c(E)$, and a peaked density of "defect" states,

$$\rho(E) = \rho_c(E) + \rho_{\text{def}}(E) . \tag{27}$$

If the defects that give rise to these states are sufficiently similar in size and nature to the holes to which the electrons are initally bound, then

$$\rho_{\text{def}}(E) \approx c_+ D_{\text{Coul}}(E) , \tag{28}$$

where c_+ is the concentration of positively charged defects. (This particularly simple example is treated in Ref. 30.) However, in general this approximate equality is not valid due to differences in the core energies of different defects. As indicated in Eq. (2) these core corrections are typically very small, but they can be of the same order of magnitude as ΔE_D and so can affect the hopping statistics dramatically. Finally, for the purposes of the detailed calculations in this section we will assume that the hopping rate between sites is of the simplest form consistent with Eqs. (3) and (4),

$$\gamma_{\vec{R}\,\vec{R}'} = \gamma_0 e^{-2|\vec{R}-\vec{R}'|/\xi} e^{-\Delta(E_{\vec{R}},E_{\vec{R}'})/k_B T} . \tag{29a}$$

where

$$\Delta(E_{\vec{R}},E_{\vec{R}'}) = \max(0, E_{\vec{R}} - E_{\vec{R}'}) , \tag{29b}$$

$E_{\vec{R}}$ is the energy of the state at site $\vec{R}$, and we have implicitly assumed that all states are of roughly the same size ξ, and have energies within about $\hbar\omega_D$ of each other.

At zero temperature, Eq. (23) is readily soluble since the electron is only permitted to hop to states with lower energy (hop down). Thus, whenever an

electron hops away from $\vec{0}$, it can never hop back. This implies that the second term in Eq. (23) is zero, and G_c is equal to

$$G_c(\hbar\omega,t)=e^{-\nu_{\rm rad}(\omega)t}\langle e^{-\Gamma_{\vec{0}}t}\rangle \ . \tag{30}$$

For hopping rates of the form given in Eq. (29), this configuration average can be performed analytically. If the density of states is featureless so that the energy of the state at site $\vec{0}$ is essentially a configuration-independent quantity, then one finds

$$G_c(\hbar\omega,t)=e^{-\nu_{\rm rad}(\omega)t}e^{-\eta(E_D)g(\gamma_0 t)} \ , \tag{31a}$$

where η is a dimensionless density of available states,

$$\eta(E_D)=\frac{\pi\xi^3}{6}\int^{E_D}\rho(\epsilon)\,d\epsilon \ , \tag{31b}$$

and g is the characteristic hopping function discussed by Scher and Lax[31,32] and by Scher and Montroll,[32]

$$g(x)=-6\sum_{n=1}^{\infty}\frac{(-x)^n}{n^3 n!}$$

$$\sim(\ln x+\zeta_E)^3+3\zeta(2)(\ln x+\zeta_E)+2\zeta(3)$$

for large x, where $\zeta_E=0.5772$ is Euler's constant, $\zeta(2)=1.645$, and $\zeta(3)=1.202$. The quantity $\eta(E_D)$ characterizes the density of available states and plays a central role in determining the hopping statistics at nonzero temperature as well as at zero temperature. To obtain a result that is more generally applicable, even when the density of states is peaked near E_D, Eq. (31a) must be averaged over the distribution of Coulombic binding energies[30]

$$G_c(\hbar\omega,t)=e^{-\nu_{\rm rad}(\omega)t}\int d\epsilon\, D_{\rm Coul}(\epsilon)e^{-\eta(\epsilon)g(\gamma_0 t)} \ . \tag{31a'}$$

At finite temperatures, Eq. (30) is valid for times small compared to the median hopping lifetime. The sum over sites that determines $\Gamma_{\vec{0}}$ must be generalized to include sites with energy greater than $E_{\vec{0}}$ since hops to sites with states higher in energy are permitted. At longer times, however, when there is a substantial probability that the electron has hopped away from $\vec{0}$, processes in which the electron hops away and then hops back become important. Since these hopping back effects always tend to increase the probability that the electron is on site $\vec{0}$, Eq. (30) can be used to calculate a lower bound to G_c at any temperature. Incorporating the effect of hop back into the calculations increases their complexity for it implies that in order to understand the process in which the electron escapes from the origin, we must also understand the processes whereby the electron can escape from the neighboring sites, once it has hopped there. For instance, an important quantity is the effective hopping-away rate from the origin $\Gamma^*_{\vec{0}}$, which is defined implicitly in terms of the mean (configuration-dependent) time the electron spends on the site $\vec{0}$,

$$(\nu_{\vec{0}}+\Gamma^*_{\vec{0}})^{-1}=\int_0^{\infty}\mathcal{G}_{\vec{0}}(t)\,dt \ . \tag{32}$$

Here $\nu_{\vec{0}}+\Gamma^*_{\vec{0}}$ is the total loss rate from site $\vec{0}$, and is equal to the sum of the effective hopping-away rate $\Gamma^*_{\vec{0}}$, and the nonhopping decay rate $\nu_{\vec{0}}$. The effective hopping-away rate can be expressed as the sum of individual effective hopping rates to neighboring sites

$$\Gamma^*_{\vec{0}}=\sum_{\vec{R}}\gamma^*_{\vec{R}\,\vec{0}} \ , \tag{33a}$$

with the individual hopping rates defined by the equation

$$\gamma^*_{\vec{R}\,\vec{0}}=\gamma_{\vec{R}\,\vec{0}}\left[1-\frac{\gamma_{\vec{0}\,\vec{R}}}{\left[\nu_{\vec{R}}+\gamma_{\vec{0}\,\vec{R}}+\sum_{\vec{R}'\neq\vec{0}}\gamma^*_{\vec{R}'\,\vec{R}}\right]}\right] \ , \tag{33b}$$

where $\gamma^*_{\vec{R}'\,\vec{R}}$ is the effective hopping rate from site $\vec{R}$ to site $\vec{R}'$. The first term on the right-hand side of Eq. (33b) is the direct hopping rate to site $\vec{R}$; the second is the correction to the effective hopping rate due to hop back.

In qualitative terms, Eq. (33) can be understood simply. If it is easy to hop from $\vec{0}$ to $\vec{R}$, but site $\vec{R}$ is isolated from other sites, i.e.,

$$\nu_{\vec{R}}+\sum_{\vec{R}'\neq\vec{0}}\gamma^*_{\vec{R}'\,\vec{R}}\ll\gamma_{\vec{0}\,\vec{R}} \ ,$$

then the most likely way to leave site $\vec{R}$ is to hop back to site $\vec{0}$ so $\gamma^*_{\vec{R}\,\vec{0}}\approx 0$. On the other hand, if site $\vec{R}$ is well connected to its surroundings i.e.,

$$\nu_{\vec{R}}+\sum_{\vec{R}'\neq\vec{0}}\gamma^*_{\vec{R}'\,\vec{R}}\gg\gamma_{\vec{0}\,\vec{R}} \ ,$$

then once the electron has hopped to site $\vec{R}$ it probably will not return to site $\vec{0}$, so $\gamma^*_{\vec{R}\,\vec{0}}\approx\gamma_{\vec{R}\,\vec{0}}$. The difficulty in solving Eqs. (33) accurately arises from the fact that in order to compute the effective hopping-away rate from site $\vec{0}$, we must know the escape rates from its neighboring sites, which in turn depend on the configuration of still

further neighbors.

We are thus led to introduce an approximation scheme which enables us to truncate this hierarchy. As certain aspects of the physics can be understood most simply in terms of this approximation we will discuss the approximation briefly and then present the results of analytic calculations performed using the approximation.

B. The greatest rate approximation

Because hopping motion in a disordered system is characterized by a broad distribution of hopping rates (see Fig. 2), the largest rate of a set of rates tends to be much larger than any of the others. The greatest rate approximation (GRA) systematizes this observation by replacing sums of rates by the largest individual rate in the sum, and the ratio of a smaller rate to a larger rate by zero. Results obtained using this approximation are expected to be asymptotically exact in the limit of an infinitely broad distribution, that is in the limit of infinitesimally small η. In the more interesting case of finite η, it yields results which generally reproduce the magnitude and the form of the functional dependences of the various quantities of physical interest.

To see how the approximation works, consider the calculation of the partial quantum efficiency $Y_{\rm ex}(\hbar\omega)$, defined in Eq. (18b). Combining the results of Eqs. (26) and (32), $Y_{\rm ex}$ can be expressed in the form

$$Y_{\rm ex}(\hbar\omega)=\int d\Gamma\left[-\frac{d}{d\Gamma}\mathscr{P}_c^{(<)}(\Gamma)\right]\times\left[\frac{\nu_{\rm rad}}{\nu_{\rm rad}+\nu_{ac}+\Gamma}\right], \tag{34}$$

where, as in Eq. (8), $\mathscr{P}_c^{(<)}(\Gamma)$ is the probability that the effective hopping-away rate from the origin [Γ_0^* in Eq. (32)] is less than Γ; hence $[-(d/d\Gamma)\mathscr{P}_c^{(<)}(\Gamma)]d\Gamma$ is the probability that the effective hopping-away rate is in the interval $(\Gamma,\Gamma+d\Gamma)$. The GRA allows us to simplify Eq. (34) in two ways. First, the ratio of rates is replaced by a step function,

$$\frac{\nu_{\rm rad}}{\nu_{\rm rad}+\nu_{ac}+\Gamma}\approx\frac{\nu_{\rm rad}}{\nu_{\rm rad}+\nu_{ac}}\Theta(\nu_{\rm rad}+\nu_{ac}-\Gamma), \tag{35}$$

so Eq. (34) can be integrated trivially,

$$Y_{\rm ex}(\hbar\omega)=\frac{\nu_{\rm rad}}{\nu_{\rm rad}+\nu_{ac}}\mathscr{P}_c^{(<)}(\nu_{\rm rad}+\nu_{ac}). \tag{34'}$$

At low temperatures, hopping is the dominant ionization mechanism ($\nu_{ac}\ll\nu_{\rm rad}$) so in effect $Y_{\rm ex}(\hbar\omega)=\mathscr{P}_c^{(<)}(\nu_{\rm rad})$. Second, the GRA simplifies the calculation of $\mathscr{P}_c^{(<)}(\Gamma)$. In Eq. (33a), Γ_0^* is expressed as a sum of effective leaving rates to individual sites $\gamma^*_{\vec{R}\,\vec{0}}$. In the GRA, $\mathscr{P}_c^{(<)}(\Gamma)$ is reinterpreted as the probability that there is no site $\vec{R}$, to which the effective hopping rate $\gamma^*_{\vec{R}\,\vec{0}}$ is greater than Γ.

With this simplification, it is easy to calculate $\mathscr{P}_c^{(<)}(\Gamma)$ at zero temperature. First, assume that the spread in Coulombic binding energies ΔE_D can be ignored so that site $\vec{0}$ has a well defined energy E_D. Since the individual hopping rates to the neighboring sites are independent of each other,

$$\mathscr{P}_c^{(<)}(\Gamma)=e^{-N^{(>)}(E_D,\Gamma)}, \tag{36}$$

where $N^{(>)}(E_D,\Gamma)$ is the mean number of sites in the neighborhood of the origin to which the hopping rate $\gamma_{\vec{R}\,\vec{0}}$ is greater than Γ. In terms of η, the dimensionless density of available sites defined in Eq. (31b),

$$N^{(>)}(E_D,\Gamma)=\eta(E_D)[\ln(\gamma_0/\Gamma)]^3. \tag{37}$$

More generally, we must average over the distribution of Coulombic binding energies. Thus, Eq. (36) should be replaced by the expression[30]

$$\mathscr{P}_c^{(<)}(\Gamma)=\int dE\,D_{\rm Coul}(E)e^{-N^{(>)}(E,\Gamma)}, \tag{36'}$$

where $D_{\rm Coul}(E)\to 0$ for $|E-E_D|\gg\Delta E_D$. Because ΔE_D is so small, $\eta(E)$ will typically vary little over an energy range of order ΔE_D if the density of states is featureless near E_D as in Fig. 4(a). In this case, Eq. (36') reduces to Eq. (36). However, if there is a high density of charged defects, resulting in a density of states peaked in the vicinity of E_D as in Fig. 4(b), Eq. (36') must be used to calculate the quantum efficiency.

Even in the context of the GRA, calculating $\mathscr{P}_c^{(<)}(\Gamma)$ as a finite temperature is a formidable task, which depends critically on the functional form of the density of states $\rho_c(E)$. However, the leading correction to Eq. (36') at low temperatures can be computed exactly in the GRA and depends only on the density of states near E_D. We will start by ignoring the distribution of Coulombic binding energies, and so obtain results that are valid if the density of states is of the featureless form shown in Fig. 4(a) (low density of charged defects). To first order in T, we find that

$$\mathscr{P}_c^{(<)}(\nu_{\rm rad})=\exp[-N^{(>)}-(T/T_0)\ln(\gamma_0/\nu_{\rm rad})\times f(N^{(>)})+O(T^2)], \tag{38}$$

where $N^{(>)}=N^{(>)}(E_D,\nu_{\rm rad})$, k_BT_0 is an energy characteristic of changes in the integrated density of states as in Eq. (20), and $f(N^{(>)})$ is a dimensionless function, computed explicitly in Appendix C [Eq. (C23)] which is negative for $N^{(>)}<0.95$ and positive for $N^{(>)}>0.95$. Thus, samples with high zero-temperature quantum efficiencies $[Y_{\rm ex}(\hbar\omega)>0.385]$ become more efficient as the temperature is increased while samples with low zero-temperature quantum efficiencies have roughly temperature-independent quantum efficiencies which have a slight tendency to decrease as a function of temperature.

To understand this behavior, first consider a system which has a rather low quantum efficiency, that is a system with $N^{(>)}>1$. Most sites have hopping-away rates greater than $\nu_{\rm rad}$. If the electron can hop away from the site $\vec{0}$ with rate greater than $\nu_{\rm rad}$ to a site $\vec{\rm R}$, it is likely that it can also escape from site $\vec{\rm R}$ with rate greater than $\nu_{\rm rad}$. Thus, even at finite temperature, the effective hopping-away rate will be greater than $\nu_{\rm rad}$. Only in the atypical configurations in which the site $\vec{0}$ is sufficiently isolated from its neighbors that the electron can never hop away before it recombines radiatively with the hole will contribute substantially to the quantum efficiency. The density of available sites increases monotonically with increasing temperature, but at low temperatures, the increase is slow. Thus, the number of isolated sites decreases slowly as a function of temperature causing a corresponding decrease in the quantum efficiency [i.e., $f(N^{(>)})$ positive]. On the other hand, if $N^{(>)}<1$ (an efficient sample) most of the sites have hopping-away rates substantially less then $\nu_{\rm rad}$, so at zero temperature, only in those configurations in which the origin has an anomalously close neighbor site $\vec{\rm R}$, will the electron manage to escape from the hole before it recombines radiatively. However, since the site $\vec{\rm R}$ is anomalously close, at finite temperatures there is a substantial probability that the hopback rate $\gamma_{\vec{0}\,\vec{\rm R}}$, which vanishes at zero temperature, is greater than the hopping rate from site $\vec{\rm R}$ to any other site. Hence, the electron is likely to hop back to the origin and the quantum efficiency *increases* with increasing temperature [i.e., $f(N^{(>)})$ negative].

The temperature-dependent quantum efficiency calculated using the GRA is shown in Fig. 5 (the solid lines) for two characteristic values of $N^{(>)}$ and $\gamma_0/\nu_{\rm rad}$, and the results are compared with the results of the computer simulation experiments described in Sec. III D. Notice particularly the inserts, where the very low temperature results

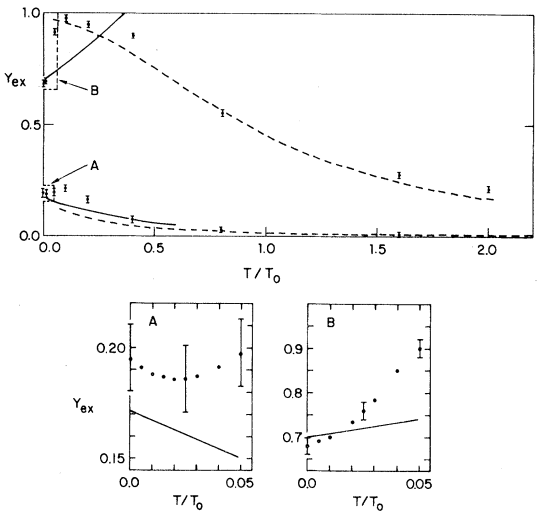

FIG. 5. Comparison between the results of the numerical simulation experiments described in Sec. III D, and the approximate analytic expressions obtained in Secs. III B and III C. The points are the results of the numerical experiments and the error bars indicate the extent of the numerical uncertainty of the results. The solid lines are the results of calculations using the GRA and the dashed lines were calculated using the TRA. In all cases, the density of states is of the form in Eq. (41a) and the hopping rates are given by the formula in Eq. (29). The inserts show the low-temperature results on an expanded scale.

$(T/T_0<0.05)$ are shown. The agreement, both in the magnitude and zero-temperature slope of the quantum efficiency, is seen to be fairly good. Although calculating the terms in Eq. (38) that are of second and higher order in the temperature is difficult, the sign of their contribution to the low-temperature quantum efficiency can be understood simply within the context of the arguments presented above. At second order in the temperature, the temperature dependence of the leaving rate $\Gamma^*_{\vec{\rm R}}$, from the nearest neighbor site to the origin, becomes important. Most often, this site will have energy less than $E_{\vec{0}}$ since most hops are still down in energy, so $N^{(>)}(E_{\vec{\rm R}})$ is generally less than $N^{(>)}(E_{\vec{0}})$. As discussed above, this implies that there is a greater tendency for hopback effects to cause $\Gamma^*_{\vec{\rm R}}$ to be a decreasing function of temperature than there is for $\Gamma^*_{\vec{0}}$. Therefore, so long as the density of available states does not increase too rapidly,

$$[\rho(E_D)k_BT]^2 \gg [\rho'(E_D)(k_BT)^2] ,$$

the first deviations from the behavior described in Eq. (38) are expected to be toward increased quan-

tum efficiency, even if the zero-temperature quantum efficiency is somewhat less than 0.385. This is indeed the behavior that is observed in both cases shown in Fig. 5.

To obtain a formula for $\mathscr{P}_c^{(>)}(\Gamma)$ that is valid for a peaked density of states of the form shown in Fig, 4(b), Eq. (38) must be averaged over possible electron binding energies

$$\mathscr{P}_c^{(<)}(\Gamma)=\int dE\, D_{\mathrm{Coul}}(E)\, e^{-N^{(>)}(E,\Gamma)} \times e^{-(T/T_0)}\ln(\gamma_0/\Gamma) f(N^{(>)}) . \tag{38'}$$

If the density of charged defects is sufficiently large that the density of states is highly peaked in the vicinity of E_D, then the quantum efficiency will generally be an increasing function of temperature at low temperature since the factor $e^{-N^{(>)}}$ in Eq. (38') heavily weights those parts of the distribution of electron binding energies for which $N^{(>)}$ is small, and hence $f(N^{(>)})$ is negative.

C. The typical rate approximation

At temperatures of order T_0 and higher the expansion in Eq. (38) breaks down and systematic calculations, even within the GRA, become very difficult. (An explicit criterion for the range of validity of the GRA is developed in Appendix C.) Moreover, since the results depend sensitively on the form of the density of states, even numerical simulation experiments are of limited value in this regime. Nevertheless, a qualitative understanding of the hopping process can be obtained in this temperature regime. We shall see that results based on this simple approximation, the typical rate approximation (TRA) developed below, are in moderately good agreement with the results of the numerical simulation experiments described in Sec. III D.

At high temperatures, despite the fact that the distribution of hopping rates is still extremely broad, the distribution of effective leaving rates is relatively narrow, so in calculating such average quantities as the quantum efficiency $Y_{\mathrm{ex}}(\hbar\omega)$, the configuration-dependent leaving rate, $\Gamma^*_{\vec{0}}$, can be replaced by a configuration-independent typical leaving rate $\tilde{\gamma}$,

$$Y_{\mathrm{ex}}(\hbar\omega)\approx\frac{\nu_{\mathrm{rad}}}{\nu_{\mathrm{rad}}+\nu_{ac}+\tilde{\gamma}} . \tag{39a}$$

To see this, consider a configuration in which the site $\vec{0}$ has an anomalously close neighbor site $\vec{R}$ ($\gamma_{\vec{0}\vec{R}}\gg\tilde{\gamma}$) which itself has effective leaving rate $\Gamma^*_{\vec{R}}=\tilde{\gamma}$. In the absence of hopping back, the electron would spend an average time $\sim\gamma^{-1}_{\vec{R}\vec{0}}$ on site $\vec{0}$. The effect of hop back is to increase this mean time, or reduce the effective leaving rate $\Gamma^*_{\vec{0}}$. If we assume that the electron can only escape via hopping to site $\vec{R}$, then the effective leaving rate, taking hop back into account is

$$\Gamma^*_{\vec{0}}=\frac{\gamma_{\vec{R}\vec{0}}\tilde{\gamma}}{\gamma_{\vec{0}\vec{R}}+\tilde{\gamma}} .$$

At high temperatures, where $\gamma_{\vec{R}\vec{0}}\sim\gamma_{\vec{0}\vec{R}}$, the leaving rate from site $\vec{0}$ will be approximately $\Gamma^*_{\vec{0}}\sim\tilde{\gamma}$. Thus the effect of hop back is to produce leaving rates on the order of the typical leaving rate regardless of the "bare" hopping rate. (Configurations in which $\gamma_{\vec{0}\vec{R}}\ll\tilde{\gamma}$ are sufficiently rare that they do not significantly affect this result.)

Of course, the details of the above analysis are not completely correct, as they are based on notions developed in the low-temperature regime where the GRA is applicable. Since the distribution of leaving rates is narrow, it is no longer permissible, as we did in the above discussion, to consider only the effective hopping rate to one "closest" neighbor site $\vec{R}$, since there may well be several sites to which the effective hopping rate is comparable. Nonetheless, the general physics of that simple discussion are in fact valid. At high temperatures, the effective leaving rate is not sensitive to the details of the local configurations about the site $\vec{0}$. In configurations in which site $\vec{0}$ has some close neighbor sites, the electron will hop many times between these close sites before diffusing away. In configurations in which the site $\vec{0}$ has no near neighbors, the electron will simply sit on the site $\vec{0}$ until it hops away. In either case, it is the rate at which the electron escapes from the neighborhood of the site $\vec{0}$ that determines the effective leaving rate, not any individual hopping rate.

There is a certain degree of arbitrariness in the choice of the typical leaving rate $\tilde{\gamma}$. $\tilde{\gamma}$ must certainly be smaller than the median hop rate γ_{med}, since even if the bare hopping rate $\gamma_{\vec{R}\vec{0}}$, from site $\vec{0}$ to site $\vec{R}$ is equal to the leaving rate from site $\vec{R}$ to the rest of the world, the effective leaving rate $\Gamma^*_{\vec{0}}$ is considerably smaller[33] than $\gamma_{\vec{R}\vec{0}}$. On the other hand, the hopping rate γ_{dc}, which determines the dc conductivity or the diffusion constant is undoubtedly smaller than $\tilde{\gamma}$, because it is dominated by the difficult hops that the electron must make to diffuse across a macroscopic system,[34,35] How-

ever, for our purposes, once the electron has escaped from the immediate vicinity of the origin it will never return. This is especially true if we consider the case in which a certain fraction of sites are nonradiative recombination centers where the electron can be annihilated as discussed in Sec. II D. $\tilde{\gamma}$ is a rate characteristic of hopping within a small cluster of sites. We have defined $\tilde{\gamma}$ as that rate for which the probability that the fastest hopping rate from site $\vec{0}$ is $\tilde{\gamma}$, is equal to the probability that the second fastest rate is $\tilde{\gamma}$. To justify this choice, let us define a cluster as a set of sites mutually connected by hopping rates greater than a defining value $\gamma_{\min}$. If we set $\gamma_{\min}=\tilde{\gamma}$ we will find small isolated clusters comprised of about one to ten sites, but as we choose smaller values for $\gamma_{\min}$, the typical size of the clusters will increase rapidly. This prescription for $\tilde{\gamma}$ yields the result

$$\tilde{\gamma}=\gamma_0\exp\{-[\eta^*(E_D,T)]^{-1/3}\}\ , \tag{39b}$$

where $\eta^*(E_D,T)$ is the effective temperature-dependent density of available states analogous to $\eta(E_D)$,

$$\eta^*(E_D,T)=\frac{\pi\xi^3}{6}\int d\epsilon\rho(\epsilon)e^{-\Delta(E,E_D)/k_BT}\ . \tag{39c}$$

To verify that this prescription is reasonable, we have checked that it satisfies the inequalities discussed above in the infinite-temperature limit where the spread in site energies can be ignored. If C_0 is the mean concentration of localized states, then

$$\begin{aligned}\ln(\gamma_{\rm med}/\gamma_0)&=-(0.79)2R_0/\xi\ ,\\ \ln(\tilde{\gamma}/\gamma_0)&=-(1.0)2R_0/\xi\ ,\\ \ln(\gamma_{DC}/\gamma_0)&=-(1.4)2R_0/\xi\ ,\end{aligned} \tag{40}$$

(see Ref. 35) where $R_0=(4\pi C_0/3)^{-1/3}$. Thus, $\tilde{\gamma}$ falls in the appropriate range. To check that the predictions of the TRA are accurate in the high-temperature regime, we have compared the prediction of Eqs. (39) with results of the numerical experiments described in Sec. III D. This comparison is summarized in Fig. 5, where the two results are seen to agree to within the accuracy of the numerical experiments.

D. Numerical simulation experiments

In order to test the validity of the approximate calculation discussed previously we have performed a series of numerical experiments on a simple class of model hopping systems.

The density of localized states to which an electron can hop is assumed to have a square-band form,

$$\rho(E)=\begin{cases}1 & \text{for } 0<E<1\\ 0 & \text{otherwise}\ ,\end{cases} \tag{41a}$$

and the density of levels induced by charged defects is given by

$$D_{\rm Coul}(E)=\frac{1}{2\Delta E_D}\times\begin{cases}1 & \text{for } |E-E_D|<\Delta E_D\\ 0 & \text{otherwise}\ ,\end{cases} \tag{41b}$$

with E_D between 0 and 1. The hopping rate between sites is calculated from Eq. (29). Thus, the statistics of the hopping motion are fully specified by the input parameters E_D, ΔE_D, the decay length ξ, the temperature T, and the radiative decay rate $\nu_{\rm rad}/\gamma_0$. For instance, the parameter $N^{(>)}$ defined in Eq. (37), which determines the zero-temperature quantum efficiency, is given by the expression

$$N^{(>)}=\frac{\pi E_D\xi^3}{6}[\ln(\gamma_0/\nu_{\rm rad})]^3\ .$$

The case of a featureless density of states such as the one shown in Fig. 4(a), can be simulated by choosing ΔE_D small and making certain that

$$e^{-(1-E_D)k_BT}\ll 1\ .$$

This latter condition ensures that the fact that the density of tail states is bounded above has minimal effect on the hopping statistics. The case of a high density of charged defects can be simulated by choosing E_D and ΔE_D equal to $\frac{1}{2}$.

In the numerical simulations, a configuration of the disordered system is generated by randomly placing 100 sites within a sphere of radius $L=(75/\pi)^{1/3}$ [which assures a unit density of sites as specified in Eq. (41a)] and associating with each site a randomly chosen site energy between 0 and 1. A site is also placed at the origin with energy randomly chosen between $E_D-\Delta E_D$ and $E_D+\Delta E_D$. The hopping rate $\gamma_{\vec{R}\,\vec{R}'}$ is computed for each pair of sites according to Eq. (29), with suitably chosen values of ξ and T. All sites within a radius $\frac{2}{3}L$ of the origin, that is in the central 30% of the volume, are considered to define the local environment of the origin, while sites in the outer 70% of the volume serve to model the medium in which the local configuration is placed. Thus, the approximation is introduced that once an electron

has hopped to a site farther than $\frac{2}{3}L$ from the origin, it will never return. The error introduced by this approximation is estimated by calculating the correction to the quantum efficiency that results from keeping terms to first order in the neglected hopping rates from distant sites (in the outer 70% of the volume) to near neighbor sites (in the inner 30% of the volume). At low temperature ($T<1$) and for all choices of the other system parameters, E_D, ΔE_D, and ξ, the error in the calculated quantum efficiency is thus estimated to be less than 5%. At higher temperatures, the neglected terms result in a systematic overestimate of the quantum efficiency which may be as large as 10—15% in the range $1<T<25$. Still higher temperature calculations will require larger sample sizes to obtain satisfactory accuracy and have not been attempted.

With this definition of the set of $\gamma_{\vec{R}\,\vec{R}'}$, Eq. (23a) is Laplace transformed as in Eq. (C1), and then solved numerically for the Laplace transform of $\mathcal{G}_{\vec{0}}(t)$. The quantum efficiency Y_{ex} is given directly in terms of the Laplace transform of $\mathcal{G}_{\vec{0}}(t)$ by Eqs. (18b), (26), and (C2). The short- and long-time behavior of $\mathcal{G}_{\vec{0}}(t)$ can also be calculated simply from its Laplace transform as discussed in Appendix C, Eqs. (C7) and (C11). The behavior at intermediate times can be estimated by interpolating between the long- and short-time forms of $\mathcal{G}_{\vec{0}}(t)$. In order to calculate the configuration average of these quantities, the entire process is repeated for 400 different configurations for each set of the system parameters. The results of some of these calculations are shown in Fig. 5 where the quantum efficiency is plotted as a function of temperature for two densities of states. The error bars mark the range of uncertainty of the experimental results due to the combined effects of hopping back from "far" sites and the statistical fluctuations expected from experiments on a finite number of configurations.

E. Hole thermalization

To study the thermalization of photogenerated holes we apply very similar considerations to those we have discussed previously for electron intersite hopping. In order to treat the general problem, the equation of motion of the site occupation probabilities [Eq. (23)] must be modified slightly by the incorporation of a source term $\mathcal{S}_{\vec{R}}$,

$$\frac{d\mathcal{G}_{\vec{R}}(t)}{dt}=-(\nu_{\vec{R}}+\Gamma_{\vec{R}})\mathcal{G}_{\vec{R}}(t)+\sum_{\vec{R}'}\gamma_{\vec{R}\,\vec{R}'}\mathcal{G}_{\vec{R}'}(t)+\mathcal{S}_{\vec{R}}(t)\,, \tag{42a}$$

where $\mathcal{S}_{\vec{R}}$ is the probability that a photogenerated hole will be captured by the state at site $\vec{R}$, and $\nu_{\vec{R}}$ is the radiative decay rate of an electron-hole pair at site $\vec{R}$. We will be interested in two physical situations: transient photoluminescence in which the holes are excited by a flash of light at $t=0$, and steady-state photoluminescence which is excited by continuous illumination. In the first case, the source term is

$$\mathcal{S}_{\vec{R}}(t)=(\text{const})(\sigma_{\vec{R}}\delta(t)\,,$$

where $\sigma_{\vec{R}}$ is the cross section for capture of holes by the state at site R, and the initial conditions are

$$\mathcal{G}_{\vec{R}}(0)=0\,.$$

In the steady-state case, the initial conditions do not matter, and the source term is

$$\mathcal{S}_{\vec{R}}=(\text{const})\sigma_{\vec{R}}\,.$$

In both cases, the quantity of interest is the configuration-averaged spectral distribution of holes defined in Eq. (8),

$$P_v(E,t)=\langle\mathcal{G}_{\vec{R}}(t)\delta(E-E_{\vec{R}})\rangle$$

$$\propto\rho_v(E)\int_0^t d\tau\left\langle\left[\mathcal{S}_{\vec{R}}(\tau)+\sum_{\vec{R}'}\gamma_{\vec{R}\,\vec{R}'}\mathcal{G}_{\vec{R}'}(\tau)\right]e^{-(\Gamma_{\vec{R}}+\nu_{\vec{R}})(t-\tau)}\right\rangle_{E_{\vec{R}}=E}\,. \tag{42b}$$

Owing to the broadness of the valence-band tail, the temperature is always small compared to the characteristic variations in the density of states, so we are always interested in hopping in the low-temperature limit. Thus, for the most part, holes will hop to a given site from a site with higher energy and leave by hopping to a site with lower energy. This implies that there is no correlation between the "hopping-on" rate and the "hopping-off" rate, so the integrand in Eq. (42) can be factored,

$$\rho_v(E)\left\langle \left[\mathscr{S}_{\vec{R}}(\tau) \sum_{\vec{R}'} \gamma_{\vec{R}\,\vec{R}'} \mathscr{G}_{\vec{R}'}(\tau) \right] e^{-\Gamma_{\vec{R}}(t-\tau)} e^{-\nu_{\vec{R}}(t-\tau)} \right\rangle_{E_{\vec{R}}=E}$$

$$\approx \rho_v(E)\left\langle \left[\mathscr{S}_{\vec{R}}(\tau) + \sum_{\vec{R}'} \gamma_{\vec{R}\,\vec{R}'} \mathscr{G}_{\vec{R}'}(\tau) \right] \right\rangle_{E_{\vec{R}}=E} \langle e^{-\Gamma_{\vec{R}}(t-\tau)} \rangle_{E_{\vec{R}}=E} e^{-\nu_{\rm rad}(E/\hbar)(t-\tau)} . \quad (43)$$

At time t, the rate at which holes reach sites with an energy E is a product of two factors: (i) the density of states $\rho_v(E)$, reflecting the number of sites with energy E, and (ii) the "site-population" rate, the average rate at which holes populate a given site $\vec{R}$, which has energy E,

$$\left\langle \left[\mathscr{S}_{\vec{R}}(t) + \sum_{\vec{R}'} \gamma_{\vec{R}\,\vec{R}'} \mathscr{G}_{\vec{R}'}(t) \right] \right\rangle_{E_{\vec{R}}=E} .$$

The resulting expression for the steady-state distribution of holes $P_{ss}(E)$ is

$$P_{ss}(E) = S(E)\rho_v(E)\left\langle \frac{1}{\Gamma_{\vec{R}} + \nu_{\vec{R}}} \right\rangle_{E_{\vec{R}}=E} ,$$

where $S(E)$ is the average site-population rate of sites with energy E. As the density of states is generally a much more rapidly varying function of energy than $S(E)$, P_{ss} is not terribly sensitive to $S(E)$. In Eq. (10b), we used the GRA to evaluate the configuration average to obtain an expression for the steady-state luminescence spectrum.

To obtain an expression for the time-dependent distribution of holes valid in transient photoluminescence experiments, we must rely on the observation that the distribution of "hopping-off" rates is much broader than the distribution of site-population rates. Thus, at times long compared to γ_0^{-1}, but shorter than $\nu_{\rm rad}^{-1}$, the variation of the hopping-off rate dependent factor in Eq. (43) can be ignored over the range of times that site-population occurs,

$$\left\langle \mathscr{S}_{\vec{R}}(\tau) + \sum_{\vec{R}'} \gamma_{\vec{R}\,\vec{R}'} G_{\vec{R}'}(\tau) \right\rangle_{E_{\vec{R}}=E} \propto S(E)\delta(\tau) .$$

In other words, a hole will hop until it finds a site sufficiently isolated that it cannot hop any more on the time scale of interest. The resulting expression for the time-dependent hole distribution is

$$P_v(E,t) = (\text{const})\rho_v(E)\langle e^{-(\Gamma_{\vec{R}} + \nu_{\vec{R}})t} \rangle .$$

Again, evaluating the configuration average using the GRA, we obtain the result quoted in Eq. (10a). Note that, consistent with the above picture of the physics of hole thermalization,

$$P_{ss}(E) \sim P_v(E, \nu_{\rm rad}^{-1}) .$$

In other words, the same physical picture applies to the steady-state case as to the transient, but in the steady-state case the time scale is set by the radiative lifetime, rather than the time at which the luminescence is observed.

Finally, because the density of valence-band tail states is large, most of the hole thermalization will be completed at times short compared to the radiative lifetime. Consider, for instance, the position of the peak energy,

$$\hbar\omega_{\rm peak}(t) \equiv E_c - E_{\rm peak}(t) ,$$

of the luminescence spectrum in Eq. (8) at time t. If we substitute Eq. (36) into Eq. (8), and differentiate with respect to energy, we obtain the implicit equation for $E_{\rm peak}(t)$,

$$\frac{d^2\eta_v(E_{\rm peak})}{dE_{\rm peak}^2} \approx \left[\frac{d\eta_v(E_{\rm peak})}{dE_{\rm peak}} \right]^2 [\ln(\gamma_0(t)]^3 , \quad (44)$$

where $\eta_v(E)$ is the dimensionless density of valence-band tail states with energy greater than E, defined analogously to $\eta(E)$ in Eq. (31b). At short times, the holes are predominantly found in states with energy near the band edge, where the density of states is large. However, once the holes have reached states with energies in a range where the density of states is low and rapidly varying, little change in $E_{\rm peak}$ will occur over many orders of magnitude of time. Thus, we were justified in treating the hole thermalization and the radiative process as independent in Eq. (17).

IV. THE POSSIBILITY FOR COMPARISON WITH EXPERIMENTS (WITH PARTICULAR REFERENCE TO *a*-Si)

To encourage the research for materials in which the photoluminescence is dominated by trapped excitons, we will conclude by summarizing the important qualitative features to be expected of such a system. The most striking features of the present model is the asymmetry in the properties of the electron and the hole. Thus, we expect such a material to have a luminescence spectrum with width

comparable to the width of the band tail, but a well-defined activation energy for dissociation of the exciton. Indeed, such an asymmetry in spectral width has been reported in hydrogenated a-Si. The luminescence spectrum is about 0.3-eV wide, while the temperature and electric field dependence of the quantum efficiency can be interpreted[5] in terms of a spread of activation energies for quenching of the luminescence of less than 0.02 eV. More recently, however, it has been shown that the same data can be interpreted differently. Thus, there is at present no compelling reason to believe that trapped excitons are important in a-Si. More direct evidence of the existence of hydrogenic exciton levels is needed to establish their existence. For instance, it may be possible to quench the luminescence with light in the infrared at an energy just sufficient to ionize the exciton.

Finally, the second possible quantitative signal of trapped exciton luminescence is the extreme sensitivity of the low-temperature quantum efficiency $\gamma(T)$, to small changes in defect concentration. In particular, for relatively efficient samples the possibility exists that $\gamma(T)$ in otherwise quite similar samples behaves qualitatively differently at low temperatures with behavior ranging from increasing with temperature to slowly decreasing with temperature. Again, although some such behavior has been observed in a-Si, its proper interpretation is not obvious.

ACKNOWLEDGMENTS

We are grateful to Professor H. Ehrenreich, Professor W. Paul, Dr. M. Paesler, Dr. A. Carlsson, Dr. D. Ling, and Dr. R. Petschek for thoughtful discussions, suggestions, and comments. This work was supported in part by the Joint Services Electronics Program Contract No. N00014-75-C-0648 and by the National Science Foundation under Grant No. DMR77-24295.

APPENDIX A: PHONON-ASSISTED ELECTRONIC TRANSITION RATES

The theory of phonon-assisted electronic transition rates has been intensively studied by many authors.[36–40] These studies, for the most part, are based on the assumption of harmonic phonons and an electron-phonon interaction that is linear in the phonon displacement. For the purpose of this paper, the details of that treatment do not matter, as the properties of interest depend logarithmically on the transition rates, so only logarithmic accuracy is required.

Let γ be the transition rate between two electronic states. Regardless of whether the process under consideration is phonon-assisted hopping, activation to the mobility edge, or nonradiative recombination, the considerations determining the rate are basically the same. First, the maximum rate at which a phonon transition can occur is determined roughly by the maximum phonon frequency, which is ω_D in the case of acoustic phonons considered here. The transition rate is generally proportional to the square of an electronic element between the two sites, of which the most important term is an electron overlap factor S. A third factor, expressing the fact that multiphonon processes are difficult, is also present. This term can be calculated exactly in a number of simple models but is generally quite complicated. If the energy difference between the two electronic states ΔE is small, however, then multiphonon processes are unimportant, especially at low temperatures, and this factor may safely be ignored. For large values of ΔE, Englemann and Jortner[38] have shown that the rate falls roughly exponentially with the average number n of phonons emitted in the process. If one or both of the electronic states is small, of order an interatomic spacing a, this average number is determined by the Debye frequency,

$$n \sim |\Delta E| / \hbar\omega_D ,$$

but for large states, Emin[39] has pointed out that only phonons with wavelength comparable to the radius ξ, of the electronic states contribute so

$$n \sim |\Delta E| / (\omega_D a / \xi) .$$

Finally, a term must always be present that expresses the condition of detailed balance. Thus, the general heuristic formula used in all our calculations for the transition rate between two electronic states is

$$\gamma = \omega_D \left[\frac{\xi_s}{\xi_l}\right]^3 e^{-2R/\xi_l} e^{-n} \times \begin{cases} 1 & \text{for } \Delta E = 0 \\ e^{-\Delta E/k_B T} & \text{for } \Delta E > 0 , \end{cases} \tag{A1}$$

where ξ_s is the radius of the smaller state, ξ_l is the radius of the larger, R is the spatial separation between the states, n is the average number of phonons involved in the process and is given by the formula above, and ΔE is the difference between the zero-phonon value of the initial- and final-state energies.

So far, we have considered only the coupling between electrons and acoustic phonons. In some amorphous insulators, especially in many systems that incorporate H, there are high-energy optical modes associated with the H. Because these modes tend to be highly localized, they will be only very weakly coupled to large electronic states, and so will not affect processes involving only large states. However, nonradiative recombination, which in our model involves rather small hole states and which is said to be suppressed by the e^{-n} term in Eq. (A1), might be highly affected by the presence of these phonons.[14]

APPENDIX B: DIPOLE-MATRIX ELEMENTS AND OVERLAP FACTORS

In this appendix, the approximate calculation of the dipole-matrix elements which determine the rate of radiative recombination is discussed [see Eqs. (12)–(14)]. Consider a large localized electron state $\phi_e(\vec{r})$, centered on the origin with radius a_e, and a hole state $\phi_h(\vec{r})$, with a much smaller radius $a_h \ll a_e$. Within the context of the effective mass approximation,[15] the electron wave function can be described in terms of an envelope function $\psi_e(\vec{R})$, and the Wannier-type tight-binding wave functions $f^{(c)}_{\vec{R}}(\vec{r}-\vec{R})$, needed to describe conduction-band edge states,

$$\phi_e(\vec{r})=\sum_{\vec{R}} \psi_e(\vec{R}) f^{(c)}_{\vec{R}}(\vec{r}-\vec{R}) , \tag{B1a}$$

where the points $\vec{R}$ are a set of atomic coordinates. If a_h is large compared to an interatomic spacing a, the hole wave function, too, can be expressed in terms of an envelope function $\psi_h(\vec{R})$, and the valence-band tight-binding orbitals $f^{(v)}_{\vec{R}}(\vec{r}-\vec{R})$,

$$\phi_h(\vec{r})\approx \sum_{\vec{R}} \psi_h(\vec{R}) f^{(v)}_{\vec{R}}(\vec{r}-\vec{R}) , \tag{B1b}$$

but if a_{hole} is comparable to a, Eq. (B1b) is not appropriate. In either case, the squared dipole matrix X^2 is given by the expression

$$X^2=\left| \int d\vec{r}\, \phi^*_e(\vec{r}) x \phi_h(\vec{r}) \right|^2 \tag{B2a}$$

$$\approx |\psi_e(\vec{0})|^2 \left| \int d\vec{r} \sum_{\vec{R}} f^{(c)}_{\vec{R}}(\vec{r}-\vec{R}) x \phi_h(\vec{r}) \right|^2 , \tag{B2b}$$

where the approximate equality in Eq. (B2b) is a consequence of the fact that $a^*_B \gg a_{\text{hole}}$. If a_{hole} is not much larger than an interatomic spacing, the integral in Eq. (B2b) does not depend sensitively on the underlying structure of the tight-binding wave functions, but only on the size of the hole wave function. Thus, the integral squared is equal to the volume of integration times a characteristic distance squared. With certainly better than order of magnitude accuracy, we can approximate the volume of integration Ω, as

$$\Omega \approx \left[\int d\vec{r}\, |\phi_h(\vec{r})| \right]^2$$

and the characteristic distance squared as the expectation value of X^2 in the hole orbital. Thus, if we assume that the wave functions are simply exponentially localized,

$$\phi_u = e^{-r/a_u}/(\pi a^3)^{1/2} , \tag{B3}$$

where $u = e$ or h, then

$$X^2 \approx (2a_h)^2 \left[\frac{2a_h}{a_e} \right]^3 \quad \text{for } a_e \gg a_h \sim a . \tag{B4}$$

In the opposite extreme, when $a_h \gg a$, the dipole matrix is proportional to a distance a_{tb}, characteristic of the size of the tight-binding orbitals,

$$X^2 \approx |\psi_e(\vec{0})|^2 |\psi_h(\vec{0})|^2 (4\pi)^2 (a_{tb})^2 ,$$

where

$$(a_{tb})^2 = \left\langle \left| \int \frac{d\vec{r}}{4\pi} \sum_{\vec{R}} f^{(c)}_{\vec{R}}(\vec{r}-\vec{R}) x f^{(v)}_{\vec{0}}(\vec{r}) \right|^2 \right\rangle$$

and $\langle\ \rangle$ denotes a configuration average. Because the tails of the tight-binding wave functions typically extend over several times the interatomic spacings, a_{tb} is generally as much as two or three times the interatomic spacing. Again, assuming the localized envelope functions are simply exponentially localized as in Eq. (B3) (see Table I)

$$X^2 \approx \frac{1}{2} \left[\frac{2a_h}{a_e} \right]^3 (2a_{tb})^2 \quad \text{for } a_e \gg a_h \gg a_{tb} . \tag{B5}$$

For greater simplicity in performing the calculations in this paper we have always used Eq. (B4) to estimate the transition rates. More properly, a formula of the form

$$X^2 \approx \left[\frac{2a_h}{a_e} \right]^3 \max[(2a_h)^2, (2a_{tb})^2] \tag{B6}$$

should be employed. However, in view of the

TABLE I. Calculated values of the squared dipole matrix. Using wave functions of the form in Eq. (B3) we calculate x^2 according to the expression in Eq. (B1), and express the results in terms of the constant C defined in Eq. (B2). The symmetry-dependent factor, $u_h^2/[(1+u_h^2)(1+u_e^2)]$, which multiplies C in all cases, has been omitted for the purposes of this table.

Hole wave function \ Electron wave function	$\exp(-r/a_B^*)$	$r^n\exp\left[-\left[\frac{(2n+4)(2n+3)}{3}\right]^{1/2}(r/a_B^*)\right]$
$\exp(-r/a_{\text{hole}})$	32	$\left[\frac{a_{\text{hole}}}{a_B^*}\right]\left[\frac{(n+2)(2n+3)}{6}\right]^{1/2}{}^n\left[\frac{2^{2n+5}}{3}\right]\left[\frac{3}{(2n+4)(2n+3)}\right]^{3/2}\frac{[(n+4)!]^2}{(2n+4)!}$
$r^n\exp\left[-\left[\frac{(2n+4)(2n+3)}{3}\right]^{1/2}(r/a_{\text{hole}})\right]$	$\frac{2^{2n+5}}{3}\left[\frac{3}{(2n+4)(2n+3)}\right]^{3/2}\frac{[(n+4)!]^2}{(2n+4)!}$	$32\left[\frac{a_{\text{hole}}}{a_B^*}\right]^n$
$\exp[-(r/2a_{\text{hole}})^2]$	1	

many uncertainties in the analysis and in particular the uncertainties regarding the exact size and shape of the localized-hole wave functions, the additional complexity does not seem warranted.

Finally, it should be noted that the formula for the dipole moment in Eq. (B3) can be used to estimate the radiative decay rates in direct gap crystals. In GaAs, for instance, the rates calculated using Eq. (B3) are found to be in good agreement with the results of more sophisticated calculations.[41]

APPENDIX C: THE STATISTICS OF HOPPING AWAY

The starting point for the calculations in this appendix is Eq. (23a). From there, the development follows a course parallel to that in Secs. III A and III B. First, via symbolic manipulations, we will derive the various formal results discussed in Sec. III. Then we will adopt the explicit form for the hopping rate in Eq. (29) and perform the various detailed calculations invoked in the text. In order to make progress with Eq. (23a), we take its Laplace transform

$$(\lambda+\nu_{\vec{R}}+\Gamma_{\vec{R}})\tilde{\mathcal{G}}_{\vec{R}\,\vec{0}}(\lambda)=\delta_{\vec{R}\,\vec{0}}+\sum_{\vec{R}'}\gamma_{\vec{R}\,\vec{R}'}\tilde{\mathcal{G}}_{\vec{R}'\,\vec{0}}(\lambda)\ , \tag{C1}$$

where $\tilde{\mathcal{G}}$ is the Laplace transform of $\mathcal{G}$,

$$\tilde{\mathcal{G}}_{\vec{R}\,\vec{0}}(\lambda)=\int_0^\infty dt\, e^{-\lambda t}\mathcal{G}_{\vec{R}\,\vec{0}}(t)\ . \tag{C2}$$

To solve this equation for $\tilde{\mathcal{G}}_{\vec{0}\,\vec{0}}(\lambda)$, we define the frequency-dependent rates

$$\Gamma^*_{\vec{R}}(\lambda)=\sum_{\vec{R}'\neq\vec{0}}\left[\gamma_{\vec{R}'\vec{R}}-\gamma_{\vec{R}\,\vec{R}'}\left[\frac{\tilde{\mathcal{G}}_{\vec{R}'\,\vec{0}}(\lambda)}{\tilde{\mathcal{G}}_{\vec{R}\,\vec{0}}(\lambda)}\right]\right], \tag{C3}$$

where $\Gamma^*_{\vec{R}}(\lambda)$ is the effective hopping-away rate to all sites excluding the origin, which we will always consider explicitly. $\Gamma^*_{\vec{R}}(\lambda)$ is the λ-dependent analogue of the effective hopping-away rate $\Gamma^*_{\vec{0}}$, defined in Eq. (32), and its physical interpretation is identical. In terms of $\Gamma^*_{\vec{R}}(\lambda)$,

$$\tilde{\mathcal{G}}_{\vec{0}\,\vec{0}}(\lambda)=\left[\lambda+\nu_{\vec{0}}+\sum_{\vec{R}}\times\left[\gamma_{\vec{R}\,\vec{0}}-\frac{\gamma_{\vec{0}\,\vec{R}}\gamma_{\vec{R}\,\vec{0}}}{[\lambda+\nu_{\vec{R}}+\gamma_{\vec{0}\,\vec{R}}+\Gamma^*_{\vec{R}}(\lambda)]}\right]\right]^{-1} \tag{C4}$$

and

$$\tilde{\mathcal{G}}_{\vec{R}}(\lambda)=\frac{\gamma_{\vec{R}\,\vec{0}}\tilde{\mathcal{G}}_{\vec{0}}(\lambda)}{\lambda+\nu_{\vec{R}}+\gamma_{\vec{0}\,\vec{R}}+\Gamma^{*}_{\vec{R}}(\lambda)} . \tag{C5}$$

Notice that the occupation probability $\tilde{\mathcal{G}}_{\vec{R}}(\lambda)$ is expressed as the ratio of the rate at which electrons hop from the origin to site $\vec{R}$, to the rate at which they escape from site $\vec{R}$. To obtain information about $\mathcal{G}_{\vec{0}}(t)$ at short times we must examine the large λ behavior of $\mathcal{G}_{\vec{0}}(\lambda)$,

$$\tilde{\mathcal{G}}_{\vec{0}}(\lambda)\sim\left[\lambda+\nu_{\vec{0}}+\sum_{\vec{R}}\gamma_{\vec{R}\,\vec{0}}-\sum_{\vec{R}}\frac{\gamma_{\vec{0}\,\vec{R}}\gamma_{\vec{R}\,\vec{0}}}{\lambda}+\cdots\right]^{-1}, \tag{C6}$$

which implies

$$\mathcal{G}_{\vec{0}}(t)=\exp\left[-\left[\nu_{\vec{0}}+\sum_{\vec{R}}\gamma_{\vec{R}\,\vec{0}}\right]t\right]\times\left[1+\tfrac{1}{2}t^{2}\sum_{\vec{R}}\gamma_{\vec{0}\,\vec{R}}\gamma_{\vec{R}\,\vec{0}}+\cdots\right] . \tag{C7}$$

This same result can be obtained directly from the equation of motion for $\mathcal{G}_{\vec{0}}(t)$ by substituting the short-time behavior of $\mathcal{G}_{\vec{R}}(t)$,

$$\mathcal{G}_{\vec{R}}(t)=\gamma_{\vec{R}\,\vec{0}}t+O(t^{2}) ,$$

into the right-hand side of Eq. (23a). The correction term,

$$\tfrac{1}{2}t^{2}\sum_{\vec{R}}\gamma_{\vec{0}\,\vec{R}}\gamma_{\vec{R}\,\vec{0}} ,$$

is thus seen to be the first hopping back correction to the direct leaving rate. At long times, the behavior of $\mathcal{G}_{\vec{0}}$ is determined by $\mathcal{G}_{\vec{0}}(\lambda)$ at small λ

$$\mathcal{G}_{\vec{0}}(\lambda)=[\nu_{\vec{0}}+\Gamma^{*}_{\vec{0}}+\lambda(1+Z)+O(\lambda^{2})]^{-1} , \tag{C8}$$

where $\Gamma^{*}_{\vec{0}}$ is the same hopping-away rate that is defined in Eq. (32), and can be written in the form

$$\Gamma^{*}_{\vec{0}}=\sum_{\vec{R}}\left[\gamma_{\vec{R}\,\vec{0}}-\frac{\gamma_{\vec{0}\,\vec{R}}\gamma_{\vec{R}\,\vec{0}}}{[\nu_{\vec{R}}+\gamma_{\vec{0}\,\vec{R}}+\Gamma^{*}_{\vec{R}}(0)]}\right] , \tag{C9}$$

and Z is defined by

$$Z=\sum_{\vec{R}}\frac{\gamma_{\vec{0}\,\vec{R}}\left[1\frac{d}{d\lambda}\Gamma^{*}_{\vec{R}}(\lambda)\Big|_{\lambda=0}\right]\gamma_{\vec{R}\,\vec{0}}}{[\nu_{\vec{R}}+\gamma_{\vec{0}\,\vec{R}}+\Gamma^{*}_{\vec{R}}(0)]^{2}} . \tag{C10}$$

Equation (C8) can be inverse Laplace transformed to yield the asymptotic form of $\mathcal{G}_{\vec{0}}$ at large t,

$$\mathcal{G}_{\vec{0}}(t)\sim\frac{1}{1+Z}\exp\left[-\frac{(\nu_{\vec{0}}+\Gamma^{*}_{\vec{0}})t}{(1+Z)}\right] . \tag{C11}$$

Equation (C11) describes a situation in which the site at the origin is in quasiequilibrium with the sites around it, spending a fraction $1/(1+Z)$ of its time on the origin and $Z/(1+Z)$ of its time on neighboring sites. This explains why the effective rate of nonhopping escape from $\vec{0}$ is reduced from its zero time value $\nu_{\vec{0}}$ by a factor $1/(1+Z)$. $\Gamma^{*}_{\vec{0}}$, as before, is an effective hopping-away rate; however, now, in order to truly escape, the electron must escape from the equilibrium region about the origin. Finally, the mean time the electron spends on site $\vec{0}$ is equal to $\tilde{\mathcal{G}}_{\vec{0}}(0)$, which confirms our interpretation of $\Gamma^{*}_{\vec{0}}$ in Eq. (21),

$$\tilde{\mathcal{G}}_{\vec{0}}(0)=(\nu_{\vec{0}}+\Gamma^{*}_{\vec{0}})^{-1} .$$

To make contact with experiment, we must calculate the configuration averages of the quantities that we have calculated for single configurations so far. At short times, because the electron leaves by all available paths independently, the configuration average of the leading term in Eq. (C7) can be evaluated rather simply,

$$\left\langle\exp\left[-\left[\nu_{\vec{0}}+\sum_{\vec{R}}\gamma_{\vec{R}\,\vec{0}}\right]t\right]\right\rangle=e^{-\nu_{\vec{0}}t}[\langle e^{-\gamma_{\vec{R}\,\vec{0}}t}\rangle]^{N}=e^{-\nu_{\vec{0}}t}[1-\langle 1-e^{-\gamma_{\vec{R}\,\vec{0}}t}\rangle]^{N} , \tag{C12}$$

where N is the number of sites in the system. For a large system, $\gamma_{\vec{R}\,\vec{0}}\approx 0$ for most configurations, hence $\langle 1-e^{-\gamma_{\vec{R}\,\vec{0}}t}\rangle$ is of order $1/N$ and in the limit $N\to\infty$,

$$(1-\langle 1-e^{-\gamma_{\vec{R}\,\vec{0}}t}\rangle)^{N}\to\exp(-N\langle 1-e^{-\gamma_{\vec{R}\,\vec{0}}t}\rangle) . \tag{C13}$$

If $\gamma_{\vec{R}\,\vec{0}}$ is given by Eq. (29), then

$$N\langle 1-e^{-\gamma_{\vec{R}\,\vec{0}}t}\rangle=\int d\vec{R}\,d\epsilon\rho(\epsilon)[1-\exp(-\gamma_{0}t\,e^{-2R/\xi-\Delta(\epsilon,E_{D})k_{B}T})] \tag{C14}$$

where

$$\Delta(\epsilon,E_D)=\begin{cases}\epsilon-E_D & \text{if } \epsilon>E_D\\ 0 & \text{if } \epsilon<E_D\ .\end{cases}$$

At zero temperature, the integral does not depend on the details of the density of states $\rho(\epsilon)$. The result is the expression in Eq. (31) of the text. At finite temperature, the integral is more sensitive to $\rho(\epsilon)$, but it can be performed rather simply for many forms of the density of states. However, this exercise is of limited usefulness, as $\mathcal{G}_{\vec{0}}(t)$ is only given by the expression in (C7) at short times, before hopback becomes important.

The GRA. To make further progress, we must introduce some approximations. In this next part, we will discuss the calculations of low-temperature properties we have evaluated using the GRA. The fundamental quantity we wish to calculate is $\mathcal{P}^{(<)}(E,\Gamma)$, the probability that the effective hopping-away rate [defined in Eq. (32)] from the site $\vec{0}$ is less than Γ, assuming that the state at site $\vec{0}$ has energy $E_{\vec{0}}=E$ for all configurations. (For the purposes of this Appendix we have made explicit the dependence of $\mathcal{P}^{(<)}$ on the energy of site $\vec{0}$, although in the text the energy dependence was suppressed for brevity.) Within the GRA, $\mathcal{P}^{(<)}$ is the probability that there is no site $\vec{R}$ to which the effective hopping rate $\gamma^{*}_{\vec{R}\,\vec{0}}$ is greater than Γ.

To get a feel for the nature of $\mathcal{P}^{(<)}(E,\Gamma)$, we will first calculate the probability $\mathcal{P}^{(<)}_{\text{bare}}(E,\Gamma)$, that there is no site $\vec{R}$ to which the "bare" hopping rate $\gamma_{\vec{R}\,\vec{0}}$ is greater than Γ. $\mathcal{P}^{(<)}_{\text{bare}}$ is equal to $\mathcal{P}^{(<)}$ at zero temperature, and at all temperatures

$$\mathcal{P}^{(<)}(E,\Gamma)\geq\mathcal{P}^{(<)}_{\text{bare}}(E,\Gamma)\ , \tag{C15}$$

since hopping back always lowers the effective leaving rates. $\mathcal{P}^{(<)}_{\text{bare}}(E,\Gamma)$ is a simple quantity to calculate since, in the limit of an infinite system ($N\to\infty$), the probability $q(E,\Gamma)d\Gamma$, that there is a site $\vec{R}$ with hopping rate $\gamma_{\vec{R}\,\vec{0}}$ in the interval $(\Gamma-d\Gamma,\Gamma)$ is independent of the number of sites to which the hopping rate is greater than Γ. Thus

$$\frac{d}{d\Gamma}\mathcal{P}^{(<)}_{\text{bare}}(E,\Gamma)=-\left[\int d\vec{R}\,d\epsilon\,\rho(\epsilon)\delta(\Gamma-\gamma_0 e^{-2R/\xi-\Delta(\epsilon,E)/k_BT})\right]\mathcal{P}^{(<)}_{\text{bare}}(E,\Gamma)\ , \tag{C16}$$

where the term in large parentheses is $q(E,\Gamma)$. Integrating Eq. (C16) we obtain

$$\mathcal{P}^{(<)}_{\text{bare}}(E,\Gamma)=\exp[-N^{(>)}_{\text{bare}}(E,\Gamma)]\ , \tag{C17}$$

where $N^{(>)}_{\text{bare}}$ is the mean number of sites to which the hopping rate is greater than Γ,

$$N^{(>)}_{\text{bare}}(E,\Gamma)=N^{(>)}+(N^{(>)}/4)[(T/T_0)\ln(\gamma_0/\Gamma)]+N^{(>)}\left[\sum_{n=1}^{\infty}\left[\frac{6\rho^{(n)}(E)(k_BT_0)^n}{n!(n+1)(n+2)(n+3)(n+4)}\right][(T/T_0)\ln(\gamma_0/\Gamma)]^{n+1}\right]\ , \tag{C18}$$

where $N^{(>)}$ is the zero-temperature value of $N^{(>)}_{\text{bare}}$. [In Eq. (37) $N^{(>)}$ is expressed in terms of the density of available states $\eta(E)$.] k_BT_0 is the logarithmic derivative of $\eta(E)$ defined in Eq. (20), and $\rho^{(n)}(E)$ is the nth derivative of $\rho(E)$. The logarithmic dependence of $\mathcal{P}^{(<)}_{\text{bare}}$ on the rate Γ is characteristic of the broad distributions of rates found in hopping systems, especially at low temperatures. We will find that, with the effect of hopping back properly accounted for within the GRA, $\mathcal{P}^{(<)}(E,\Gamma)$ is given by the expression in Eq. (38) which is of the same form as the expression for $\mathcal{P}^{(<)}_{\text{bare}}$ in Eqs. (C17) and (C18), however, with the factor of $(N^{(>)}/4)$ in Eq. (C18) replaced by a characteristic function $f[N^{(>)}(E,\Gamma)]$.

To see this first consider the expression for the effective hopping rate to site $\vec{R}$ given by Eq. (33b). We distinguish two classes of sites, "near" sites which are in closer contact with site $\vec{0}$ than with the rest of the world, $\Gamma^{*}_{\vec{R}}<\gamma_{\vec{0}\,\vec{R}}$, and "far" sites which are in closer contact with the rest of the world than with $\vec{0}$, $\Gamma^{*}_{\vec{R}}>\gamma_{\vec{0}\,\vec{R}}$. (Note, since we are interested in low temperatures, the rate at which electrons are thermally activated to E_c is small. Thus, in this part of the appendix we will let $\nu_{\vec{R}}=\nu_{ac}\approx 0$ for $\vec{R}\neq\vec{0}$.) Within the GRA,

$$\mathcal{P}^{(<)}(E,\Gamma)=\mathcal{P}^{(\text{far})}(E,\Gamma)\mathcal{P}^{(\text{near})}(E,\Gamma)\ , \tag{C19}$$

where $\mathcal{P}^{(\text{far})}$ is the probability that there is no far site for which $\gamma^{*}_{\vec{R}\,\vec{0}}>\Gamma$, and $\mathcal{P}^{(\text{near})}$ is the probability that there is no near site with $\gamma^{*}_{\vec{R}\,\vec{0}}>\Gamma$. Moreover, the expression for $\gamma^{*}_{\vec{R}\,\vec{0}}$ is also simplified by the GRA,

$$\gamma^*_{\vec{R}\,\vec{0}}=\gamma_{\vec{R}\,\vec{0}}\times\begin{cases}1 & \text{if } \gamma_{\vec{0}\,\vec{R}}<\Gamma^*_{\vec{R}}\\ \dfrac{\Gamma^*_{\vec{R}}}{\gamma_{\vec{0}\,\vec{R}}} & \text{if } \gamma_{\vec{0}\,\vec{R}}>\Gamma^*_{\vec{R}}\end{cases}. \tag{C20}$$

At finite temperature, hops involving several sites contribute to the effective hopping rate, so it is no longer necessarily true that the probability $q^*(E,\Gamma)d\Gamma$ of finding a site to which the effective rate is in the interval $(\Gamma-d\Gamma,\Gamma)$ is independent of the number of sites N, to which the effective hopping rate is greater than Γ. However, in an infinite system, q^* is not very strongly dependent on N for N small (the range of physical interest). Moreover, to lowest order in the temperature, or within the GRA at all temperatures, q^* is, in fact, completely independent of N. Thus, just as with $\mathcal{P}^{(<)}_{\text{bare}}$, it follows that $\mathcal{P}^{(\text{near})}$ falls exponentially with the mean number of near sites, $N^{(\text{near})}(E,\Gamma)$, to which the effective hopping rate is greater than Γ. $\mathcal{P}^{(\text{far})}$ depends analogously on $N^{(\text{far})}$. Together with the result in expression (C19), this implies

$$\mathcal{P}(E,\Gamma)=\exp[-N^{(\text{near})}(E,\Gamma)-N^{(\text{far})}(E,\Gamma)]$$

where, from Eqs. (C20)

$$N^{(\text{near})}(E,\Gamma)=\int d\vec{R}\,d\epsilon\rho(\epsilon)\int d\gamma\left[-\frac{d}{d\gamma}\mathcal{P}^{(<)}(\epsilon,\gamma)\right]\delta(\Gamma-\gamma e^{-|E-\epsilon|/k_BT})\Theta(\gamma_0 e^{-2R/\xi-\Delta(E,\epsilon)/k_BT}-\gamma), \tag{C21}$$

and

$$N^{(\text{far})}(E,\Gamma)=\int d\vec{R}\,d\epsilon\rho(\epsilon)\int d\gamma\left[-\frac{d}{d\gamma}\mathcal{P}^{(<)}(\epsilon,\gamma)\right]\times\delta(\Gamma-\gamma_0 e^{-2R/\xi-\Delta(\epsilon,E)/k_BT})\Theta(\gamma-\gamma_0 e^{-2R/\xi-\Delta(E,\epsilon)/k_BT}). \tag{C22}$$

In these expressions, the term $-(d/d\gamma)\mathcal{P}^{(<)}(\epsilon,\gamma)$ is the probability that the effective leaving rate from the site $\vec{R}$ is in the range $[\gamma,\gamma+d\gamma]$. Equations (C21) and (C22) are complicated integral equations for $\mathcal{P}^{(<)}(E,\Gamma)$ in terms of itself. In general, there is no good way to solve these equations. However, to first order in the temperature, the zero-temperature expression for $\mathcal{P}^{(<)}(\epsilon,\Gamma)$ can be used to evaluate the integrals on the right-hand side (r.h.s) of Eqs. (C21) and (C22). Corrections to the effective hopping rate from site $\vec{0}$ to site $\vec{R}$ due to the temperature dependence of the effective leaving rate from site $\vec{R}$ appear first in second order.

With this simplication it is straightforward to evaluate the integrals. The result is expressed in Eq. (38). The characteristic function $f(x)$ is given by the expression

$$f(x)=\left[\frac{x}{4}+xe^{-x}+\frac{g_{1/3}(x)(x-1/3)-(1/3)!x}{x^{2/3}}\right], \tag{C23}$$

where $g_{1/3}(x)$ is the incomplete gamma function,

$$g_{1/3}(x)=\int_0^x y^{1/3}e^{-y}dy, \tag{C24}$$

and $(1/3)!$ is the gamma function of $-2/3$, $(1/3)!=g_{1/3}(\infty)$. For small argument, $x\ll 1$, $f(x)$ is negative,

$$f(x)=-(1/3)!x^{1/3}+x+\cdots, \tag{C25}$$

while for large argument, $x\gg 1$, $f(x)$ is positive,

$$f(x)\sim\frac{x}{4}-\frac{(1/3)!x^{-2/3}}{3}. \tag{C26}$$

Of particular importance is the value of the argument $x_0=0.95$, where $f(x)$ changes sign, since this marks the line between those values of the parameters for which the quantum efficiency is an increasing or decreasing function of temperature.

Finally, a criterion must be developed to determine the range of temperatures over which the expansion of $N^{(>)}$ to first order in T is useful. Rather than performing the complicated numerical integrations necessary to calculate the second term in the expansion, we can use the second-order term in the expansion of $N^{(>)}_{\text{bare}}$ to estimate the size of the higher-order effects. Typically, the terms in the expansion of $N^{(>)}_{\text{bare}}$ are larger in magnitude than those in the expansion of $N^{(>)}$. Thus, the expression in Eq. (38) is probably valid so long as

$$(T/T_0)\ln(\gamma_0/\Gamma)\ll\frac{120f(N^{(>)})}{\rho'(E)k_BT_0}. \tag{C27}$$

*Present address: Physics Department, SUNY at Stony Brook, Stony Brook, NY 11973.
†Present address: IBM Thomas J. Watson Research Center, Yorktown Heights, NY 10598.

[1]D. G. Thomas, J. J. Hopfield, and W. M. Augustyniak, Phys. Rev. 140, A202 (1965).
[2]Some of the early evidence for the existence of tails of tailing states in heavily doped crystalline semiconductors came from photoluminescence experiments. See B. I. Halperin and M. Lax, Phys. Rev. 1448, 722 (1966), Ref. 3.
[3]D. G. Thomas, M. Gershenzon, and J. J. Hopfield, Phys. Rev. 131, 2397 (1963); Y. Yafet and D. G. Thomas, *ibid.* 131, 2405 (1963).
[4]A good list of references, as well as an up-to-date summary of the experimental situation is hydrogenated *a*-Si, is contained in M. A. Paesler and W. Paul, Philos. Mag. (in press).
[5]M. A. Paesler and W. Paul, Philos. Mag. (in press).
[6]D. Engemann, and R. Fischer, in *Proceedings of the Seventh International Conference on Amorphous and Liquid Semiconductors, University of Edinburgh, Edinburgh, 1977,* edited by W. E. Spear (Edinburgh University, Edinburgh, 1977), p. 387.
[7]I. G. Austin, T. S. Nashashibi, T. M. Searle, P. G. LeComber, and W. E. Spear, J. Non-Cryst. Solids 32, 373 (1979).
[8]T. M. Searle, T. S. Nashashibi, and I. G. Austin, Philos. Mag. B 37, 389 (1979).
[9]C. Tsang, and R. A. Street, Phys. Rev. B 19, 3027 (1979).
[10]R. A. Street, Adv. Phys. 25, 397 (1976).
[11]K. Morigaki, D. J. Dunstant, B. C. Cavenett, P. Dawson, J. E. Nicholls, S. Nitta, and K. Shimakawa, Solid State Commun. 26, 981 (1978).
[12]R. A. Street, D. K. Beigelsen, J. C. Knights, C. Tsang, and R. M. White, *1978 Conference on Thin Films, Southampton, 1978* (in press).
[13]G. S. Higashi and M. Kastner, Phys. Rev. Lett. 47, 124 (1981).
[14]N. F. Mott, Philos. Mag. 36, 413 (1977).
[15]S. Kivelson and C. D. Gelatt, Phys. Rev. B 19, 5160 (1979).
[16]S. Kivelson and C. D. Gelatt, Phys. Rev. B 20, 4167 (1979), and unpublished.
[17]W. E. Spear, Adv. Phys. 26, 312 (1977).
[18]J. C. Knights, T. M. Hayes, and J. C. Mikkelson, Jr. Phys. Rev. Lett. 39, 712 (1977).
[19]This argument is based on the assumptions that the electron travels an average distance $\bar{l}$ between each phonon emission, when it loses all memory of its previous motion, and that with each emission it gives up an average energy of order $\hbar\omega_D$. It is similar to the argument presented by Engemann and Fischer in Ref. 6. However, they use the macroscopic diffusion constant to determine the length $\bar{l}$. This often leads to an estimated $\bar{l}$ that is less than an interatomic spacing. The use of a macroscopic diffusion constant over such short distances is certainly not justified.
[20]It should be noted that even at fixed, low-excitation energy, this process is not really simply exponentially activated, since a distribution of electron-hole separations exist with spread of order l_{relax}. Thus, ϵ_{in} in Eq. (6c) should be viewed as defining a characteristic temperature ϵ_{in}/k_B, rather than a well-defined activation energy. At higher excitation energies, the amount of excess energy lost by the electron and hole during thermalization $E-E_{\text{gap}}$ is considerable, so local heating effects may be important and T in Eq. (6b) should be considered a local temperature which may be considerably higher than the ambient. As both the local temperature and l_{relax} are increasing functions of excitation energy ν_{ex} is also an increasing function. However, its precise excitation energy dependence may be quite complicated.
[21]B. I. Halperin and M. Lax, Phys. Rev. 1448, 722 (1966).
[22]L. I. Schiff, *Quantum Mechanics* (McGraw-Hill, New York, 1949), p. 255.
[23]Even if the density of states is "highly asymmetric," there is a slight correlation between the electron and hole hopping, since the effective radiative recombination rate depends on the electron hopping motion at nonzero temperature [see Eq. (C11)]. However, as the hopping statistics depend logarithmically on the radiative decay rate, the differences in the effective radiative decay rates due to different local configurations of localized conduction-band states do not often have a significant effect on the hole statistics. Moreover, most of the hole thermalization takes place much faster than the radiative lifetime, so the electron and hole processes are essentially independent, even at nonzero temperatures.
[24]ΔE_D is determined by a combination of two effects: (1) differences in the local environment produce small differences in the binding energy of an electron bound to a point charge, and (2) differences in the nature of the hole to which the electron is bound produce a spread in core corrections to the energy. In general, these two effects are comparable in magntiude. For *a*-Si it is estimated in Ref. 15 that the environment produced spread in energies is about $\Delta E_D \sim 0.015$ eV. The total core correction to the binding energy due to the presence of a phosphorous is also estimated in Ref. 15, and is found to be about the same size, $\Delta E_{\text{core}} \sim 0.02$ eV. We would expect the spread in core energies due to differences in the hole orbitals to be somewhat less than this. Therefore, in *a*-Si, we find that ΔE_D is predominantly a measure of the spread in local environments characteristic of the disordered structure.
[25]For instance, the lifetime of carriers in photoconductivity experiments is usually determined by recombination at deep defect levels, or "recombination centers." See A. Rose, *Concepts in Photoconductivity and Allied Problems* (Interscience, New York, 1963).

[26]In some cases, much less restrictive conditions can be placed on the intensity while still insuring that all radiative recombination is germinant. At low temperatures, once an electron has found its way to a state with energy more than a few times k_BT less than E_D, it will not be able to hop to the localized state bound to the hole. Thus it will either recombine nonradiatively or, possibly, by some lower-energy radiative process. An example of such a lower-energy radiative process may be the 0.8-eV luminescence line sometimes observed in hydrogenated a-Si (see Ref. 7).

[27]H. Fritzche, in *Amorphous and Liquid Semiconductors,* edited by J. Tauc (Plenum, London, 1974), p. 221.

[28]Consider a system with N charged defects of either sign. The median exciton-ionization rate due to electrons hopping to impurity-related states is roughly $\tilde{\gamma}=\gamma_0 e^{-2R_0/a_B^*}$, where $R_0=(4\pi/3N)^{-1/3}$. Since γ_0 is typically several orders of magnitude greater than $\nu_{\rm rad}$, the quantum efficiency will be essentially zero if $2R_0 \sim a_B^*$. Thus, for luminescent samples, the separation between charges must be much greater than a_B^*. However, as the holes are quite immobile, the effects of the negatively charged centers will only become important when $R_0 \sim a_B^*$. Thus, we conclude that the effect of positively charged defects is always much greater than the effect of negatively charged defects.

[29]W. Y. Ching, D. J. Lam, and C. C. Lin, Phys. Rev. Lett. 42, 805 (1979).

[30]If, as in Eq. (28), we assume that $\rho_{\rm def}(E)=c_+ D_{\rm Coul}(E)$, and if we further assume that the integrated density of "intrinsic" tail states,

$$\eta_c(E)=\int^E \rho_c(\epsilon)d\epsilon\ ,$$

does not vary much for energies E, in the range $E_D-\Delta E_D \lesssim E \lesssim E_D+\Delta E_D$, then the averaging of the various quantities discussed in Secs. III A and III B over the distribution of Coulombic binding energies $D_{\rm Coul}(E)$ can be performed analytically. Thus, $G_c(\hbar\omega,t)$ in Eq. (31a′) becomes

$$G_c(\hbar\omega,t)=e^{-\nu_{\rm rad}(\hbar\omega,t)}e^{-\eta_c(E_D)g(\gamma_0 t)} \times(1-e^{-\eta_{\rm def}\, g(\gamma_0 t)})/\eta_{\rm def}\, g(\gamma_0 t)\ ,$$

where $\eta_{\rm def}=\pi(a_B^*)^3 c_+/6$. Similarly, Eq. (36′) for $\mathscr{P}_c^{(<)}(\Gamma)$, which determines the quantum efficiency, becomes

$$\mathscr{P}_c^{(<)}(\Gamma)=e^{-\eta_c(E_D)[\ln(\gamma_0/\Gamma)]^3} \times(1-e^{-\eta_{\rm def}[\ln(\gamma_0/\Gamma)]^3})\{\eta_{\rm def}[\ln(\gamma_0/\Gamma)]^3\}^{-1}\ .$$

The striking aspect of these results is that charged defects of this sort have relatively little effect on the luminescence signal. Whereas the quantum efficiency falls exponentially with increasing density of available tail states $\eta_c(E_D)$, it falls off only with the first power of $\eta_{\rm def}$. This conclusion depends sensitively on the fact that the centroid of the distribution of "defect" states coincides with the centroid of the distribution of photoinduced states. A small difference in the core energies of the two types of states can enormously affect the results due to the extreme narrowness of the distributions. If the defect states lie a few times ΔE_D above the photoinduced states, then they will have essentially no effect on the luminescence. If they lie a few times ΔE_D below the photoinduced states, then they contribute an exponential dependence similar to $\eta_c(E_D)$.

[31]H. Scher and M. Lax, Phys. Rev. B 7, 4491 (1973); 7, 4502 (1973).

[32]H. Scher and E. Montroll, Phys. Rev. B 12, 2455 (1975).

[33]To see this, consider the crystalline case, in which the leaving rate from each site is equal to $\gamma_{\rm med}$. Owing to the effect of hopping back, the effective leaving rate $\tilde{\gamma}$ is always less than $\gamma_{\rm med}$, although the exact ratio of $\tilde{\gamma}/\gamma_{\rm med}$ depends on both the coordination number and the dimensionality of the lattice [see, for example, E. W. Montroll and G. H. Weis, J. Math. Phys. 6, 167, (1965)]. In one dimension, and some two-dimensional lattices, the electron always returns to the origin. Although we are considering three-dimensional disordered systems since each site has one or two near neighbors to which the hopping rate is much greater than to any others, locally the system appears to have a lower dimensionality and the effect of hopping back is greater than is normally expected of three-dimensional lattices.

[34]V. Ambegaokar, B. I. Halperin, and J. S. Langer, Phys. Rev. B 4, 2612 (1976).

[35]P. N. Butcher, K. J. Hayden, J. A. McInness, Philos. Mag. 36, 19 (1977); C. H. Seager and G. E. Pike, Phys. Rev. B 10, 1435 (1974).

[36]I. G. Austin and N. F. Mott, Adv. Phys. 18, 41 (1969).

[37]T. Holstein, Philos. Mag. B 37, 49 and 499 (1978).

[38]R. Engemann and J. Jortner, Mol. Phys. 18, 145 (1978).

[39]D. Emin, Phys. Rev. Lett. 32, 303 (1974).

[40]T. Holstein, Ann. Phys. (N.Y.) 8, 325 and 343 (1959); E. Gorham-Bergeron and D. Emin, Phys. Rev. B 15, 3667 (1977); Y. Weissman and J. Jortner, Philos. Mag. B 37, 21 (1978).

[41]G. C. Osbourn and D. L. Smith, Phys. Rev. B 20, 1556 (1979).